The Term Structure of Macroeconomic Risks at the Effective Lower Bound

Guillaume ROUSSELLET*

First version: January 2017 This version: June 2021

Abstract

This paper proposes a new macro-finance model that solves the tension between tractability, flexibility in macroeconomic dynamics, and consistency of the term structures of treasury yields with the effective lower bound (ELB). I use the term structures of U.S. nominal and real treasury yields from 1990 to explore the interdependence between inflation expectations, volatility, and monetary policy at the ELB. The estimation reveals that real yields stay elevated during the ELB due to large premia and deflation fears, produced by a persistent shift in inflation dynamics, with low average inflation and heightened inflation volatility.

JEL Codes: C58, E43, G12

Key-words: Affine Term Structure Model, Effective Lower Bound, QTSM, TIPS, Liftoff Probabilities, Inflation Risk Premia.

*McGill University – Desautels School of Management, 1001 Sherbrooke St. West, Montreal QC H3A 1G5, CANADA, guillaume.roussellet@mcgill.ca

1 Introduction

During the last decade, U.S. short-term interest rates have shown an unprecedented behavior being stuck at their effective lower bound (ELB henceforth) for an exceptionally long period. As conventional monetary policy easing becomes unfeasible, questions emerge on the central bank's ability to escape the deflation trap and stimulate the economy. At the heart of this debate is the idea that the ELB is a fundamentally different state of the world where the relationship between interest rates and macroeconomic outcomes cannot be understood using pre-ELB data (see e.g., the discussion between Cochrane (2017) and Christiano (2017)). Models adapted to pre- and post-ELB periods are therefore central for monetary policymakers, as they are key to understand if real yields are elevated because of prolonged expected deflation, large risk premia, or both, and provide the appropriate policy (in)action.

While existing macro-finance models can guide these policy questions, they must address conflicting challenges. On the one hand, traditional *affine* models provide flexible representations of yields and macroeconomic variables through elegant pricing formulas. However, they have difficulties reproducing a short-term interest rate bounded from below, or its ability to stay at the lower bound for long periods (Andreasen and Meldrum 2018), which limit their utility for policymakers confronted to a long-lasting ELB. On the other hand, while *shadow-rate* models tackle the ELB-consistency successfully, it is at the expense of tractability. Moreover, this class of models show limited flexibility in macroeconomic dynamics with, for instance, stochastic volatility (see e.g., Kim and Singleton (2012)), such that they behave as a fully Gaussian model away from the ELB. Yet, each of these ingredients is critical to paint an accurate empirical picture of monetary policy and macroeconomic interdependence during the ELB (Fernandez-Villaverde and Rubio-Ramírez 2007; Coibon and Gorodnichenko 2011).

In this paper, I address the tension between tractability, ELB-consistency, and flexibility by introducing a new macro-finance framework that captures macroeco-

nomic and treasury curves dynamics at the ELB. I exploit the model to investigate the potential change in inflation dynamics when the economy reaches the ELB, the pricing of inflation components, and the policy response in such a low-yield environment. In my model, inflation dynamics are driven by expectation and volatility shocks, both of which are priced by investors. As a result, these shocks are reflected in long-maturity bond yields, risk premia, and in the likelihood of a binding ELB, even when the monetary policy rate is persistently stuck at its lower bound. A particular feature of the model is that it does not assume an exogenous regime shift when the ELB starts binding, but rather uses information available throughout the pre- and post-ELB samples jointly to identify pricing relationships. Being able to provide an explicit link between inflation factors and sovereign yields during the ELB salvages the informativeness of yields and extends the traditional macro-finance models *à la* Ang and Piazzesi (2003).

Despite featuring nonlinearities, my model is particularly easy to handle because it belongs to the so-called *affine* class. First, nominal and real yields at any maturity are obtained as closed-form functions of state variables, including inflation components. All nominal yields are consistent with the ELB, and the short rate can be persistently stuck there. Second, inflation and yields' expectations and volatility forecasts are available in closed form. Third, probabilities to stay at the ELB or to lift off are explicitly driven by the state variables. The availability of the above moments opens the door for survey data to be included in the estimation. Fifth, impulse-response functions are non-linear and state-dependent, but computable easily, allowing for an easy comparison of pre- and post-ELB results. Last, all observables are at most linear-quadratic combinations of the states, which greatly simplifies estimation with the quadratic filter of Monfort, Renne, and Roussellet (2015) as opposed to particle filtering as in e.g. Fernandez-Villaverde and Rubio-Ramírez (2007). The estimation is then performed with pricing targets of 1- to 10-year maturity nominal and real U.S. treasury yields observed monthly from 1990 to 2015, along with inflation and survey

data.

The estimation provides three main takeaways. First, treasury yield curves uncover the existence of adverse inflation outcomes during the ELB period. Inflation trend and volatility filtered from the model show persistently large undershooting and overshooting, respectively, compared to the pre-ELB period. Looking at the pricing of inflation components, I show that these outcomes translate into large premia that drives elevated real yields. As the inflation central tendency falls and inflation uncertainty increases, deflation fears arise at short-maturities (-190bps). While these deflation fears are limited at longer maturities, nominal premia grow with maturity, from virtually zero at 1y to between 100bps and 350bps during the ELB period for the 10y bond. In contrast, the expectation components are small and slowly moving so that lowering real yields can mostly come from lowering its premia. This result contrasts with low or negative nominal term premia commonly implied by affine models, which can be an artifact of a fast model-implied mean-reversion from the ELB.

Second, a non-linear impulse-response analysis reveals that a monetary policy shock produces more diverse and uncertain effects during a binding ELB period compared to normal times. I find that from 1990 up to 2011 effects of tightening monetary policy shocks are fairly homogenous. Inflation expectations go slightly up, and inflation risk premia decreases in reaction, but the overall effects are moderate. In turn, short-term yields stay elevated persistently leading to an overall increase in nominal and real yield curves. Surprisingly, from 2012 onwards, the effects on both inflation and financial outcomes reverse. Lifting off by a few basis points immediately leads back to the ELB since such a shock was highly improbable at the time, which decreases real yields by nearly 10 basis points across the curve. This shifting point happens a few months after the introduction of calendar-based forward guidance, when investors' expectations about the length of the ELB became well-anchored as the probability to stay at the ELB for one-year went above 90%. Investors' expectations can thus largely influence the effect of monetary policy responses.

Third, I provide evidence that the monetary policy response to "*embrace the ELB*" (Williams (2009)) and to delay the increase of short-term rates (i.e. the liftoff) was in line with investors' perceptions. I derive the risk premium associated with a synthetic digital bond, paying off only if the economy is still at the ELB at maturity. I find that this asset is considered a hedge by investors, and its premium is negative. A further decomposition provides evidence that this fear is substantially driven by inflation trend and volatility shocks, a previously undocumented result which complements the findings of Breach et al. (2020). I show that these premia become more negative after unconventional monetary policy events, especially after QE2 These policies can contribute to investors' perception of the ELB, and lead them to prefer to delay the exit from the ELB.

This paper gathers both a modeling and an empirical innovation relative to the existing literature. First, for the former, the new term structure model introduced below combines tractability for pricing nominal and real Treasuries, for the joint dynamics of their yields with macroeconomic components, as well as the ability to enforce a sticky effective lower bound. The affine is preserved by combining the non-negative gamma-zero process of Monfort et al. (2017) to represent the ELB-consistent short rate, with a standard quadratic term structure framework, which is known for its empirical performance (see Ahn, Dittmar, and Gallant (2002), Leippold and Wu (2007)).[1] The estimated model shows appealing empirical properties, with low pricing errors on both nominal and real term structures (3bps and 12bps on average, respectively) with only four factors, and generates a substantially higher probability to stay at the lower bound compared to a standard QTSM. As such, it complements the important study of Andreasen and Meldrum (2018) by expanding the range of available ELB-consistent affine models.

Other approaches have been considered to produce an ELB-consistent pricing

1. Alternative ELB-consistent models include Filipovic, Larsson, and Trolle (2017) linear-rational term structure model, Feunou, Fontaine, Le, and Lundblad (2015) nearly arbitrage-free framework and Renne (2014) discrete states model.

framework. The shadow-rate approach enforces the ELB and constitutes an alternative to the present model, stepping outside the class of affine models (see e.g. Kim and Singleton (2012)).[2] These models usually pose a challenge at the estimation stage, since pricing has to be approximate and show limited flexibility.[3] Conversely, by staying in the affine world, my model can be estimated quickly even incorporating macroeconomic and yields forecasts, as well as proxies for liftoff probabilities, in the set of empirical targets. This strengthens the identification of the joint macroeconomic and financial dynamics at virtually no cost, a particularly important feature when yields show limited variability at the ELB.

Second, my paper contributes to a strand of empirical literature devoted to understanding the dynamics of inflation through the study of nominal and real treasuries. Numerous term structure models have been developed to extract inflation dynamics and inflation pricing from asset prices (see e.g. Barr and Campbell (1997), Evans (1998), or Anderson and Sleath (2001)). However, most papers either do not consider ELB-consistency (Haubrich et al. (2012) or Fleckenstein et al. (2017)), are focused on the estimation of the relative liquidity of real bonds (e.g. Grischenko and Huang (2013), Abrahams et al. (2016), or D'Amico et al. (2018)) or are focused on inflation dynamics pre-ELB binding period (see Ang et al. (2008) Adrian and Wu (2009), and Campbell et al. (2017)). In contrast, the empirical exercise in this paper focuses on the potential change of interdependence between inflation components and asset prices in and out of the ELB. As such, it builds on the insights of both Mertens and Williams (2018) and King (2019) that a non-linear model is needed to understand the shift implied by an economy stuck at the ELB.

2. Examples include and are not limited to Lemke and Vladu (2016), or Andreasen and Meldrum (2015) for yield-only models, Bauer and Rudebusch (2016), or Wu and Xia (2016) for macro-finance models. Carriero et al. (2018) employ a shadow rate model on nominal and real term structures jointly. Branger et al. (2016) incorporate a shadow rate in a long-run-risk model with inflation dynamics.

3. Approximate estimation methods for SR models have been developed by Kim and Priebsch (2013), Priebsch (2013), Wu and Xia (2016) and Christensen and Rudebusch (2015). Computationally intensive algorithms are also provided by Andreasen and Meldrum (2011) and Pericoli and Taboga (2015).

Last, this paper has implications for the literature looking at the relevance of the effective lower bound for macroeconomic models (see Gali (2018) for a survey of New Keynesian models). My empirical results resonate with the debate between Aruoba, Cuba-Borda, and Schorfheide (2017) and Reichlin (2015), on whether the ELB created a shift to a deflation equilibrium driven by expectation shocks. I find that inflation dynamics are indeed modified at the ELB, and that the anchoring of ELB expectations matter for the effect of monetary policy shocks. Cochrane (2017) advocates that none of the stark predictions of standard macroeconomic models on inflation are validated during the ELB period, and proposes a new model based on fiscal theory. Debortoli, Gali, and Gambetti (2020) show the irrelevance of the ELB for macroeconomic impulse-responses through a time-varying VAR. In turn, papers looking at asset prices show that there is a significant link between inflation components and treasury curves (see e.g. Ehling, Gallmeyer, and Heyerdahl-Larsen (2018)), a moderate but significant change in inflation densities when the ELB is binding (see Mertens and Williams (2018)), or a change of correlation of inflation with stock returns (Gourio and Ngo (2020)) during the ELB. My paper contributes to this debate by trying to extract information about inflation dynamics from asset prices using a reduced-form model, hence not taking a stand on the structural assumptions underlying the above works.

The remainder of the paper is organized as follows. Section 2 presents the formulation and the properties of the term structure model. I present the identification strategy and estimation method in Section 3, along with the fitting properties of the model. Section 4 presents the empirical results. Section 5 concludes.

2 A model for inflation risks and interest rates

I introduce the joint asset pricing model for nominal and real yields and observable macroeconomic factors. While I formulate it directly with inflation dynamics, a more

general specification is presented in internet Appendix B.1. I specify the pricing factors physical dynamics and express the nominal pricing kernel such that all yields are closed-form functions of the factors. Importantly, the framework imposes a lower bound for the nominal term structure.

2.1 Inflation central tendency and stochastic volatility

I assume that the dynamics of a $K \times 1$ vector of risk factors X_t are given by the following vector autoregression:

$$X_{t+1} = \mu + \Phi X_t + v_{t+1}\,, \tag{1}$$

where $v_{t+1} \overset{i.i.d.}{\sim} \mathcal{N}(0, \Sigma)$. This state vector contains three sets of variables, such that $X_{t+1} = \left(\pi^*_{t+1},\, \sigma_{t+1},\, y'_{t+1}\right)'$ where both π^*_{t+1} and σ_{t+1} are univariate and y_t is a vector of yield-specific risk factors of size $K_y \times 1$.

Inflation is defined as the year-on-year log-change of the CPI-U index, denoted by CPI_{t+1}, such that $\pi_{t+1} = \log(\text{CPI}_{t+1}/\text{CPI}_{t-11})$. Inflation dynamics are driven by the first two elements of X_{t+1}, and the inflation rate is given by:

$$\pi_{t+1} = \bar{\pi} + \pi^*_t + \sigma_{t+1}\varepsilon^{\pi}_{t+1}\,, \tag{2}$$

where $\varepsilon^{\pi}_{t+1} \overset{i.i.d.}{\sim} \mathcal{N}(0,1)$, and is uncorrelated with v_{t+1}. Equation (2) has two key features drawn from the literature on modeling and forecasting inflation. First, π^*_t is the time-varying component of expected inflation and can be interpreted as the inflation central tendency (or conditional mean, see e.g. Feunou and Fontaine (2014)), representing its low frequency fluctuations. Second, σ_{t+1} is the stochastic volatility of inflation thus reproducing its high frequency fluctuations.[4]

4. Motivation for time-varying volatility and short- and long-run components of inflation can be found among others in Engle (1982), Stock and Watson (2007), Cogley, Primiceri, and Sargent (2010), or Garcia and Poon (2018). An alternative specification for σ_{t+1} could be an independent Gamma process as in Haubrich, Pennacchi, and Ritchken (2012). This would ensure positivity of

2.2 An ELB-consistent short-rate specification with macroeconomic factors

In this economy, there exists a riskless n-maturity nominal investment accessible to investors at time t at price $P_t^{(n)}$. The one-month riskless yield is known at t and given by $r_t = -\log P_t^{(1)}$. Assuming no-arbitrage, r_t cannot in principle become negative since investors would just hoard cash otherwise, thus is bounded by the zero lower bound. In practice, there is an effective lower bound $\underline{r}$ that can differ from zero and the observed yield evolves above this ELB. Figure 1, left panel, presents the time series of the one-year nominal yield, and emphasizes the important stickiness of the ELB, from 2009 to the end of our sample in 2015.

To reproduce these features, I assume that the short-term yield is given by:

$$r_t = \underline{r} + z_t \,, \tag{3}$$

where z_t is a univariate non-negative stochastic process whose dynamics are given by the autoregressive gamma-zero introduced by Monfort et al. (2017). These dynamics are defined through a mixing Poisson variable P_t, such that:

$$\mathsf{P}_t \,\big|\, (X_t,\, z_{t-1}) \sim \mathcal{P}\left(\alpha + \phi z_{t-1} + \kappa \beta' X_t + (\beta' X_t)^2\right) \quad \text{and} \quad z_t \,\big|\, \mathsf{P}_t \sim \Gamma\left(\mathsf{P}_t\,;\, c\right) \,, \tag{4}$$

where ϕ, κ, c and α are positive scalars, β is of dimension $K \times 1$, and P_t is the degree of freedom of the gamma distribution.[5]

I obtain several implications from this specification. First, z_t is equal to zero as long as the Poisson draws P_t are equal to zero. This allows the short-rate process r_t to reach its lower bound $\underline{r}$ and potentially spend long periods there. Second, even though I allow only one linear combination of the state vector to enter the Poisson

the process but would lose the potential feedback effects with the other elements of X_t to preserve the closed-form pricing expressions in our context. The empirical impact of such a choice is left for future research.

5. A sufficient condition for the intensity being positive is that $\alpha = \frac{\kappa^2}{4}$.

intensity for parsimony, the specification is general enough such that inflation mean and volatility factors π_t^* and σ_t as well as yield-specific factors y_t all impact the current one-period yield. As noted by Andreasen and Meldrum (2018) in the context of a standard quadratic model, this specification is supported by data and is barely restrictive. Last, the probabilities of reaching or getting away from the lower bound crucially depend on the current values of both inflation and yield-specific risk factors, namely X_t. The remaining properties of the gamma-zero distribution are detailed in Appendix A.1.

2.3 Short-rate dynamics: discussion

Our specification shares some features with quadratic term structure models (QTSM, see e.g. Ahn et al. (2002) or Breach et al. (2020)) However, Equation (4) defines a short-rate able to stay at the ELB, contrary to QTSMs. One key distinction of the model with respect to a standard QTSM is that it directly enables to identify periods when the lower bound $\underline{r}$ is binding, i.e. when realizations of z_t are equal to zero.

Additionally, my model allows for the time-varying Taylor rule feature of Ang et al. (2011), with monetary policy shifts. To gain some insight, Let us consider a simple case where X_t consists only of the inflation trend π_t^* with zero mean, and where the ELB is zero. We can write:

$$r_t = \overline{r} + \underbrace{\rho \cdot r_{t-1}}_{\text{smoothing}} + (1-\rho) \underbrace{\left[1 + \frac{\beta}{\kappa}\pi_t^*\right] \frac{c\kappa\beta}{1-\rho}}_{\text{policy shift}} \pi_t^* + \varepsilon_t^z \,, \tag{5}$$

where ε_t^z a zero-mean martingale difference sequence conditionally on π_t^* and r_{t-1}. We can interpret the coefficients of the model in light of Equation (5). The coefficient $\frac{c\kappa\beta}{1-\rho}$ constitutes the baseline reaction of monetary policy to inflation expectation movements when inflation expectations are on target ($\pi_t^* = 0$). When the expectations deviate from target, monetary policymakers adjust their reaction function

depending on how far the economy is from the steady state. It is easy to calculate the immediate response of the short-rate to a positive inflation shock ε, given by $\beta^2\varepsilon^2 + [\kappa\beta + 2\beta^2\mathbb{E}_{t-1}(\pi_t^*)]\varepsilon$. We can directly see that the policy reaction is positively correlated with inflation expectations, a feature validated by data (see Figure 3 of Ang et al. (2011)), and consistent with the asymmetric policy response proposed by Bianchi et al. (2019).

To bring additional insights, we simulate the policy rule given by Equation (5), where the parameters are obtained by matching means, covariances, and autocorrelations of inflation and the 3m Tbill rate over the 1990-2015 sample. We obtain the results presented on Figure 2. Inflation starts at its 2.3% steady state and drops by 30bps over the first 5 years of the simulation and stays persistently low (Panel a). On panel (b), the resulting short rate drops during the first 10 years of the simulation. Since inflation expectations are dragging persistently down, the short-rate reaches the ELB after 14 years and stays there for about 7 years, a duration empirically relevant. When at the ELB, inflation has a significant impact on the probability to stay there. We see on panel (c) that because it is still too low compared to the steady state, the probability to be at the ELB for another year is above 75% (black solid line), while it would be 70% if inflation was on target. Last, the monetary policy shifts can also be observed on the right axis of panel (a). The response to a 1% increase in inflation expectations is 1.7 when the economy is at the steady-state, and drops below 1.5 before the economy reaches the ELB.

[Include Figure 2 about here.]

Last, notice that the general framework can readily include any measure of real activity in addition to inflation series to obtain a more standard Taylor rule specification. While this could bring additional insights to the interpretation of the model's empirical estimates, I choose to focus primarily on inflation dynamics and let the latent yield factors adapt to fitting the yield curve and predicting inflation at low and high frequencies.

2.4 The pricing kernel

I assume that the pricing kernel of the representative investor M_{t+1} is given by an exponential-affine function of the shocks to the risk factors:

$$M_{t+1} = \exp\left(- r_t + \lambda_t' \, v_{t+1} + \lambda_r \, [r_{t+1} - \mathbb{E}_t(r_{t+1})] - \xi_t \right) \tag{6}$$

where $\mathbb{E}_t(\bullet)$ is the conditional expectation operator given the filtration spanned by the history of $\{X_t, \pi_t, z_t\}$, and ξ_t is the convexity adjustment such that $\mathbb{E}_t\left(M_{t+1}\right) = e^{-r_t}$ (see Appendix A.1 and Internet Appendix B.3 for their respective form). As in Duffee (2002), the prices of risk are in the essentially affine form:

$$\lambda_t = \lambda_0 + \lambda_1 X_t \, . \tag{7}$$

Equation (6) emphasizes that both inflation trend and volatility shocks are priced. As usual with this type of kernel, investors attribute a price λ_t to shocks v_{t+1}, and empirical estimates usually reflect that they fear positive inflation shocks. However, a second channel is at play when investors price unexpected shocks to the short rate. The latter is driven by squares of the Gaussian shocks v_{t+1}, and investors also price large deviations to their inflation components forecasts, whatever their sign (see also Appendix A.1). Such a channel is consistent with two-sided fears of inflation as documented for instance in Kitsul and Wright (2013).[6]

Despite the non-linearities in the pricing kernel specification, I show in Appendix A.2 that it has a self-preserving structure hence the risk-neutral dynamics of the risk factors are given by:

$$X_{t+1} = \mu^{\mathbb{Q}} + \Phi^{\mathbb{Q}} X_t + v_{t+1}^{\mathbb{Q}} \, , \tag{8}$$

6. Note that it is possible to impose that inflation risks are unspanned by the nominal yield curve through linear constraints on the prices of risk and on the parameters driving the joint dynamics of yield-specific and inflation factors (see Joslin et al. (2014))

where $v_{t+1}^{\mathbb{Q}} \overset{i.i.d.}{\sim} \mathcal{N}\left(0, \Sigma^{\mathbb{Q}}\right)$ and:

$$\begin{aligned}
\mu^{\mathbb{Q}} &= \left(I_K - 2\frac{\lambda_r c}{1-\lambda_r c}\Sigma\beta\beta'\right)^{-1}\left(\mu + \Sigma\lambda_0 + \frac{\kappa\lambda_r c}{1-\lambda_r c}\Sigma\beta\right) \\
\Phi^{\mathbb{Q}} &= \left(I_K - 2\frac{\lambda_r c}{1-\lambda_r c}\Sigma\beta\beta'\right)^{-1}\left(\Phi + \Sigma\lambda_1\right) \\
\Sigma^{\mathbb{Q}} &= \left(I_K - 2\frac{\lambda_r c}{1-\lambda_r c}\Sigma\beta\beta'\right)^{-1}\Sigma\,.
\end{aligned} \tag{9}$$

The risk-neutral dynamics of the short-rate factor z_t is then given by:

$$z_t \,\big|\, X_t,\, z_{t-1} \overset{\mathbb{Q}}{\sim} \text{ARG}_0\left(\alpha^{\mathbb{Q}} + \phi^{\mathbb{Q}} z_{t-1} + \kappa^{\mathbb{Q}}\beta^{\mathbb{Q}\prime} X_t + \left(\beta^{\mathbb{Q}\prime} X_t\right)^2 ;\, c^{\mathbb{Q}}\right), \tag{10}$$

where $\alpha^{\mathbb{Q}}$, $\phi^{\mathbb{Q}}$ and $c^{\mathbb{Q}}$ are equal to their physical counterparts divided by $(1-\lambda_r c)$, and both $\kappa^{\mathbb{Q}}$ and $\beta^{\mathbb{Q}}$ are equal to their physical counterparts divided by $\sqrt{1-\lambda_r c}$.

2.5 Pricing the term structures

By no-arbitrage, the prices of nominal bonds of any maturity n are given by:

$$P_t^{(n)} = \mathbb{E}_t^{\mathbb{Q}}\left[\exp\left(-\sum_{i=0}^{n-1} r_{t+i}\right)\right], \tag{11}$$

where $\mathbb{E}_t^{\mathbb{Q}}(\bullet)$ is the risk-neutral conditional expectation operator given the filtration spanned by the history of $\{X_t,\, \pi_t,\, r_t\}$. In contrast, inflation-protected securities (TIPS hereafter) are securities paying off at maturity the realized inflation from issuance to maturity. For any maturity n, their prices are given by:[7]

$$P_t^{(n)^*} = \mathbb{E}_t^{\mathbb{Q}}\left[\exp\left(-\sum_{i=0}^{n-1} r_{t+i}\right)\frac{\text{CPI}_{t+n}}{\text{CPI}_t}\right], \tag{12}$$

7. I discuss the specifics of TIPS in the Section detailing the data, notably our treatment of the so-called inflation lag used to compute the actual payoff of TIPS.

Despite the non-Gaussian structure of the framework, I show in Appendix A.2 that the risk-neutral dynamics of inflation, of the risk factors and of the short-rate obtained in the previous Section define an affine-quadratic term structure model (ATSM-QTSM) where the pricing Equations (11) and (12) can be obtained through closed-form recursions:

$$\begin{aligned} P_t^{(n)} &= \exp\left(\mathcal{A}_n + \mathcal{B}_n' X_t + X_t' \mathcal{C}_n X_t + \mathcal{D}_n z_t\right), \\ P_t^{(n)^*} &= \exp\left(\mathcal{A}_n^* + \mathcal{B}_n^{*\prime} X_t + X_t' \mathcal{C}_n^* X_t + \mathcal{D}_n^* z_t\right). \end{aligned} \tag{13}$$

The explicit recursions are functions of the risk-neutral parameters and are detailed in Appendix A.3. Corresponding continuously-compounded nominal and real yields are given by $R_t^{(n)} := -\frac{1}{n}\log P_t^{(n)}$ and $R_t^{(n)^*} := -\frac{1}{n}\log P_t^{(n)^*}$, respectively, and are linear-quadratic combinations of the risk factors.

The fact that the model belongs to the class of QTSMs allows for several extremely useful features. Contrary to the shadow-rate model, I do not need to rely on any approximation or simulation technique to obtain the term structures since the pricing formulas are analytic (see for instance Wu and Xia (2016) or Christensen and Rudebusch (2015)). Second, the combination of physical and risk-neutral dynamics imply that forecasts of yields of all maturities at all horizons are obtained as closed-form linear-quadratic combinations of the risk factors (see Internet Appendix B.5). Although the previous properties are usually available in a standard QTSM, the gamma-zero distribution properties provide the conditional probabilities to stay at the ELB for any length n as a closed-form function of the factors:

$$\mathbb{P}_t\left(r_{t+1:t+n} = \underline{r}\right) = \exp\left(\mathcal{A}_n^{\mathbb{P},(\text{elb})} + \mathcal{B}_n^{\mathbb{P},(\text{elb})\prime} X_t + X_t' \mathcal{C}_n^{\mathbb{P},(\text{elb})} X_t + \mathcal{D}_n^{\mathbb{P},(\text{elb})} z_t\right), \tag{14}$$

where the loadings are given through closed-form recursions in Appendix A.4. These two points prove particularly useful in practice for improving the quality of the estimation through the use of forecast data, both for yields levels and liftoff probabilities (see e.g. Kim and Orphanides (2012)). I include both in the empirical application

below.

3 Estimation Strategy

3.1 Identification strategy and data

I consider monthly U.S. data from January 1990 to March 2015.We obtain the one-month nominal interest rate from Bloomberg (<*GB1M Index*>) and longer nominal zero-coupon yields for maturities of 1, 2, 3, 5, 7, and 10 years from Gurkaynak et al. (2007). For TIPS, I compute liquidity-adjusted synthetic yields by subtracting zero-coupon inflation swap rates of maturities of 1, 2, 3, 5, 7, and 10 years obtained from Bloomberg (<*USSWITx Crncy*>, converted to continuous compounding) to the corresponding-maturity nominal bond (see Christensen and Gillan (2012) or Moench and Vladu (2018)).[8] The inflation-linked swap data starts in July 2004. I treat the months following Lehman failure – from September 2008 to February 2009 – as missing data since most movements on the TIPS interest rates during this period can likely be attributed to the disruption of the inflation-indexed market (see for instance D'Amico et al. (2018)). The year-on-year inflation rate is computed from the CPI-U series of the BLS database, and is lagged of 3 months to be consistent with the reference price index.

[Include Figure 1 and Table 1 about here.]

To better identify the joint dynamics of yields and inflation, I follow Kim and Orphanides (2012) and Chernov and Mueller (2012) adding two sets of survey forecasts in the observable variables. I obtain series of expected average inflation over the next

8. Christensen and Gillan (2012) note that though not free from liquidity risk, inflation swaps are less likely to be affected by liquidity issues compared to TIPS (see also Fleckenstein et al. (2017)). For papers who focus on extracting the liquidity risk from TIPS data, see for instance Sack and Elasser (2004), Shen (2006), Gurkaynak et al. (2010), Grischenko and Huang (2013), Pflueger and Viceira (2016) or D'Amico et al. (2018). Fleckenstein et al. (2014) note that the TIPS bonds were also subject to large mispricing during the crisis.

1 and 10 years and nominal yields forecasts for the 10-year maturity, respectively 3-months and 1-year ahead from the Philadelphia Fed database. All these surveys are quarterly. Last, I extract data about the probabilities of seeing no interest rate increase by the Fed between each date and one year ahead from the primary dealer survey conducted by the New York Fed. I collect information starting from January 2011. Details on these computations are provided in internet Appendix B.7. Time series and standard descriptive statistics of interest rates and inflation are presented in Figure 1 and in Table 1. Surveys and ELB probability series are represented in Figure 3.

3.2 The state-space formulation

All the observables except two are closed-form linear-quadratic combinations of the state variables X_t and z_t. On the one hand, the probabilities to stay at the ELB are exponential linear-quadratic functions of the states (see Equation (14)). I therefore take the natural logarithm of the probabilities data. On the other hand, inflation dynamics involve the i.i.d. shocks ε_t^π and the lag of π_t^* which are not readily included in our state variables VAR. I take care of this issue augmenting the states as $X_t^{(aug)} = (X_t', \varepsilon_t^\pi, \pi_{t-1}^*)'$ without changing their VAR structure.

$$X_t^{(aug)} = \begin{pmatrix} X_t \\ \varepsilon_t^\pi \\ \pi_{t-1}^* \end{pmatrix} = \begin{pmatrix} \mu \\ 0 \\ 0 \end{pmatrix} + \begin{pmatrix} \Phi & 0 & 0 \\ 0 & 0 & 0 \\ e_1' & 0 & 0 \end{pmatrix} \begin{pmatrix} X_{t-1} \\ \varepsilon_{t-1}^\pi \\ \pi_{t-2}^* \end{pmatrix} + \begin{pmatrix} I & 0 \\ 0 & 1 \\ 0 & 0 \end{pmatrix} \begin{pmatrix} v_t \\ \varepsilon_t^\pi \end{pmatrix}, \tag{15}$$

where e_1 the first column of the identity matrix.

I now turn to the state-space formulation of the model. To fix ideas, consider that all our observables at time t are gathered in a vector denoted by $\mathcal{Y}_t^{(obs)}$. This vector contains all 13 yields, the inflation rate, 4 inflation and yields survey series and one ELB log-probabilities series. I assume that all these observables except inflation are

measured with errors, and write:

$$\mathcal{Y}_t^{(obs)} = \mathcal{A} + \mathcal{B}' X_t^{(aug)} + \mathcal{C}\,\text{Vec}\left(X_t^{(aug)} X_t^{(aug)'}\right) + \mathcal{D}\, z_t + \eta_t\,, \tag{16}$$

where each element of η_t is independent and $\eta_{i,t} \overset{i.i.d.}{\sim} \mathcal{N}(0, \omega_i^2)$ are the measurement errors. For parsimony, I assume the the standard deviation of the measurement errors is the same across nominal yields on the one hand, across TIPS yields on the other hand, and calibrated to the average forecaster disagreement.

I consider 2 latent yield-specific factors y_t ($K_y = 2$). Without further assumptions, the latent factors can still be rotated and are not uniquely identified (see for instance Joslin et al. (2011)). I therefore impose several constraints on the parameters driving the dynamics of our risk factors. The conditional covariance matrix Σ is diagonal and the part corresponding to y_t is set to identity. I impose that the autoregressive matrix Φ is upper triangular so all factors can feedback on π_t^*. For identification, I also impose that the model-implied mean of π_t^* is null so that average inflation is given directly by $\bar{\pi}$.

Since the measurement equations (16) are linear-quadratic in the states and all states form an affine process, I can readily estimate the model using the *Quadratic Kalman filter* of Monfort et al. (2015). The method allows to take care of the quadratic part of the state-space model more efficiently than standard approximate non-linear filters such as the extended and unscented Kalman filters, although the latter methods could be used as well. The algorithm is detailed in internet Appendix B.6. Alternatively, the sequential regression approach of Andreasen and Christensen (2015) could be used for estimation since the model is affine. In any case, these methods allows for one likelihood call in less that 1 second on a standard computer, facilitating numerical issues compared to particle filtering, the standard method for evaluating complex likelihoods (see e.g. Fernandez-Villaverde and Rubio-Ramírez (2007)).

I perform a first estimation with the previous constraints and set all non-significant

parameters to zero for a second round, and repeat until all parameters are significant.

3.3 Model validation: estimates and fitting properties

The estimated parameters are presented on Tables 3 and 4 in the Appendix. Inflation central tendency has persistence of 0.89, and inflation volatility of 0.98. Estimates of β show that the central bank reacts to inflation trend shocks ($\beta_{\pi^*} = 0.05$) but not significantly to inflation volatility, thus caring primarily about medium/long-run inflation (see Table 4). Under the risk-neutral measure, inflation volatility has and receives feedback from all the other risk factors including inflation trend. It therefore plays a significant role in the pricing of both nominal bonds and TIPS of long maturities through risk premia.

[Insert Table 2 and Figure 3 about here.]

The model is able to provide both a reasonable fit on the SPF data that is tracking down closely the quarterly series (see Figure 3), and an impressive fit on both term structures with only 4 factors. RMSEs range from 2bps to 5bps for nominal rates and from 6bps to 17bps for real rates (see Table 2). These fitting properties are comparable to the model of Abrahams et al. (2016), who use a 5-factor ATSM to fit both yield curves. In comparison, my model only has 4 factors, two of which are identified by inflation dynamics. Quadratic models are well-known to fit yields more efficiently than a pure linear model with the same number of factors (see e.g. Leippold and Wu (2007)).

To confirm the added value of the ELB-consistency in addition to the quadratic structure of my framework, I estimate a standard QTSM without the gamma-zero variable but with the same structure as presented in Section 2. In essence, the estimated QTSM is very close to the one in Andreasen and Meldrum (2018) or Breach, D'amico, and Orphanides (2020) but adding the fact that yields should be positive. I replace Equations (3) and (4) by: $r_t = \underline{r} + \kappa\beta' X_t + (\beta' X_t)^2$. I focus on the stickiness

of the ELB for both models by simulating data using the estimated parameters from both models to compare the probabilities of obtaining interest rates below 25bps. The difference is striking: the Gamma-QTSM model implies a 28% probability to reach the ELB and a 30% probability to obtain a short-term interest rate below 25bps while the standard QTSM-implied probability for staying below 25bps is only 9%. This reflects on the decomposition of nominal rates: the standard QTSM-implied expected components are consistently higher and more volatile than for our model. This shows that the standard QTSM cannot generate enough persistence at the ELB. This complements the analysis of Andreasen and Meldrum (2018), showing that adding a gamma-zero variable to the standard QTSM can solve some of its inconsistencies during the ELB.

Last, I check that both objective and risk-neutral dynamics are well-identified by performing the LPY tests of Dai and Singleton (2002)[9]. Models relying on positive processes usually have difficulties passing these tests (see e.g. Backus et al. (2001)). Conversely, Figure 11 and Table 6 of the internet Appendix show that both conditions cannot be rejected at the 5% level, thus validating the empirical estimates.

4 Empirical Results

4.1 Inflation dynamics at the lower bound

An important question that has arisen in the macroeconomic debate is whether reaching the ELB fundamentally changes inflation dynamics. The estimated model provides a natural answer to that question by using both inflation data and a large cross-section of treasury yields to back out inflation trend and volatility time series, hence strengthening their identification. The filtered factors are presented on Figure 4, along with the date at which the the ELB starts binding.

[Insert Figure 4 about here.]

9. see internet appendix B.8 for details about these tests in the present setting.

The estimated inflation central tendency and volatility both exhibit a large shift at the ELB, pointing towards a change in inflation dynamics. The inflation trend π_t^* mostly fluctuates around zero between 1990 and 2009, jumps to $\pi_t^* = -4\%$ in 2009, leading to an inflation forecast of $\overline{\pi} + \pi_t^* = -1.16\%$. It stays consistently in the negative territory afterwards. At the end of the sample, the filtered π_t^* is close to -3%, producing an overall inflation forecast of about 0%. A similar phenomenon can be seen for inflation volatility, which is comprised below 1% before the ELB starts binding, but spikes up to 3% and stays elevated afterwards.

The identification of inflation components through bond yields reveals that the ELB episode in the U.S. resulted in persistent adverse inflation shocks, where inflation stayed below target with a large volatility during the five ELB-binding years included in the sample. This empirical evidence supports the view that the ELB resulted in a prolonged low inflation/deflation regime at the ELB, and a potential shift to a different equilibrium (Aruoba et al. 2017). These stylized facts are hard to identify using historical inflation data only as in e.g. Debortoli et al. (2020), but can be efficiently unveiled by the use of asset prices. The ELB-consistency is key to identify these features of inflation volatility.

4.2 Why are real interest rates high at the ELB?

While the short-term nominal rate is stuck at the ELB, long-term rates continue to move in accordance with the state variables, including inflation shocks. The prolonged low inflation trend observed at the ELB pushes real yields upward, slowing down the recovery. Swanson and Williams (2014) argue that these long-term rates have been virtually unaffected by the ELB, possibly because of nominal and inflation term premia responsiveness to news occurring during the period. Whether yields are dominated by risk premia rather than expectations is an empirical question, which warrants a different monetary policy action depending on the answer.

I first ask whether the shift of inflation trend and volatility at the ELB can explain

the fact that real yields stayed elevated. The sensitivities – or loadings – of yields to the different factors are presented on Figure 5.

[Insert Figure 5 about here.]

Looking at Figure 5, we see that inflation central tendency is nearly unpriced in the nominal term structure (left panel), and is priced negatively in real yields (middle panel). Thus, the sudden drop in the inflation trend is soaked up by increasing real yields, with virtually no impact on nominal bonds. Second, inflation volatility is one of the most important factors to explain nominal and real yields' fluctuations, especially at medium-run maturities (diamonds symbols on Figure 5). For the 5-year yield for instance, the linear loading associated with σ_t is the most important, at par with that of the latent factor $y_{1,t}$, and ranks close second for the quadratic loadings. The increase in inflation volatility when the economy hit the ELB further pushed real yields upwards.

However, most of these increases are driven by risk premia rather than expectations. Decomposing the loadings of each yields in expectation and risk premium component on Figure 6, I dissect the effects of adverse inflation outcomes on yields. First, the TIPS reaction to the inflation trend is affecting the expected future real yields and risk premium roughly the same for the whole term structure. Second, inflation volatility does not cause any of the other factors and does not enter the monetary policy rule (see parameter estimates in Table 3 and 4) so its impact on bond yields can only go through term premia, not the expectation component. In the end, most of the shift in inflation dynamics gets reflected in investors' risk aversion, thus explaining the substantial movements of long-run yields despite a slowly-moving expectation component.

[Insert Figure 6 about here.]

To investigate more precisely the behavior of these premia during the ELB, I provide the historical decomposition of expectation and risk premia components ob-

served during the ELB period on Figure 7. The behavior of the 1-year nominal yield post-crisis reflects the persistence of the ELB-binding period. The 1-year and 10-year expectation components become virtually null and below 100bps, respectively. The latter is nearly constant through time, emphasizing the stability of investors expectations that short-term interest rates will remain low for a long period of time. This leads most of the nominal yields fluctuations to be explained by the term premium that investors require to hold these bonds. During the ELB period, the 1-year nominal risk premia component is null whereas most of the 10-year nominal term premium is consistently positive and volatile, fluctuating between 100bps and 350bps. Most of the responsiveness of the long-run nominal yields during the ELB can therefore be attributed to fluctuations in the term premium.

[Insert Figure 7 about here.]

On the inflation risk premia series (IRP, right panel of Figure 7), the empirical estimates show inverted patterns compared to nominal term premia. At the short-end, the ELB coincides with a surge in deflation fears where the IRP reaches an all time low of nearly -200bps. The post-2009 period shows a convergence to close-to-zero historical values but the inflation risk premium stays consistently negative between 0 and -60bps. Conversely, the 10-year inflation premium component has a low volatility, and slowly fluctuates around 0. When the ELB hits, the long-run IRP also peaks down but to a moderate -60bps before converging to positive historical values.

Translating these to real components by subtracting nominal and inflation components, the U.S. experienced heightened short-term yields not only because of a drop in inflation expectations, but because of significant short-run deflation fears. At the ELB, the 1y TIPS yields would have reached -1.5% absent deflation fears compared to 0% historically. At the long-end, the containment of deflation fears plays favorably for real yields. However, notably through increased inflation volatility, nominal uncertainty is significant and drives 10y real yields upwards.

4.3 Discussion of the risk premium estimates

Risk premia estimates are only as good as the term structure model. While I have confirmed previously that the fitting properties of my model were satisfactory, it is useful to compare the risk premium estimates to previous literature to gain some perspective. Fleckenstein et al. (2017) estimate a positive and stable 1-y inflation premium (IRP henceforth), contained between 0bps and 30bps on a 2009/2015 sample. In comparison, their 10-y inflation premium is very volatile, peaking at 80bps in January 2010 and going to negative territory at −35bps from early 2015 onwards. Haubrich et al. (2012) imposes risk premia estimates to be functions of the conditional volatility of interest rates only. This produces long-term real term premia and inflation risk premia that are roughly constant over time and consistently positive. Abrahams et al. (2016) produce obtain a 10-y IRP fluctuating between −40bps and 90bps from 2000 to 2014. Breach et al. (2020) find a 2y and 10y IRP negative during the ELB period (about −50bps) but more pronounced business cycle fluctuations. These existing studies attribute both a different sign and magnitude to IRP since they all gather different modeling features.

In comparison my model combines several of these features altogether such as including inflation expectations data and inflation stochastic volatility. The IRP estimates provided above show a time-series behavior consistent with Abrahams et al. (2016) and overall magnitudes consistent with Breach et al. (2020). The sign of my IRP estimates are particularly in line with the model-free estimates of Camba-Mendez and Werner (2017). However, the ELB constraint on nominal yields is unique to my framework and uncovers the particular pattern of a large dip detailed above, with a larger volatility for the short-run IRP.

4.4 The effect of monetary policy shocks at the lower bound

With high real risk premia, a natural question to ask is whether monetary policy can help getting out of the deflation trap and push down real yields to stimulate the

economy. In particular, Aruoba et al. (2017) suggest that lifting-off from the ELB may increase inflation expectations and allow the economy to escape the deflation state, mostly through the Fisher effect. While this counterintuitive effect is debated by Reichlin (2015), the effect of monetary policy shocks at the ELB lacks empirical evidence. I investigate policy responses below.

I derive impulse-response functions to observe the effect of an exogenous liftoff shock on inflation components and asset prices in the economy. Note that the model inherently embeds nonlinear dynamics through the short rate specification (4). Both magnitude and sign of impulse-responses thus critically depend on the starting state. This property is conform with the fact that the ELB represents a fundamentally different regime and that the reaction of asset prices to the exact same shocks can be different in normal times and during the ELB (Lansing 2020, for instance). A key advantage of the framework is that impulse-responses for each of these variables of interest are obtained in closed-form.

I perform impulse-responses resulting from a tightening monetary policy shock starting from each date in the sample. To make sure that the liftoff shock is independent from inflation shocks, I impose that it is fully reflected by shocks to the yield-specific factors y_t. The size of the shock is equal to the conditional volatility of the short-term interest rate at the starting date. These tightening/liftoff shocks range from 1bps to 17bps, and average 12bps before the ELB-binding period, and about 3bps afterwards. After a first pass, I uncovered a certain homogeneity of the IRFs over three sub-periods: *(i)* pre-ELB, *(ii)* unanchored ELB-binding [2009-2011] and *(iii)* anchored ELB-binding [2012-2015]. I grouped the results accordingly and computed the median, min and max responses over these sub-periods. The entire methodology is detailed in Appendix A.5, and Figure 8 presents its results.

[Insert Figure 8 about here.]

The IRFs show different features depending on the considered subsample. In normal times, a tightening monetary policy shock tends to be accompanied by further in-

creases up to 30bps after a year, and slowly decays afterwards. This shock raises the term structure mostly through the expectation component so the yield curve flattens. Inflation expectations increase by only 1bp, while both short and long-run inflation risk premia go down by 2bps, and inflation volatility slightly decrease. These are fairly moderate effects with respect to the size of the initial tightening policy shock, and shows that monetary policy had low impact on inflation components, in particular inflation volatility.

A binding ELB produces two distinct effects that are present during the unanchored and anchored periods. The former produces qualitatively the same effects as when the ELB is not binding, but has a wider uncertainty. The size of the initial shock produces a maximum of 20bps on the short-term interest rate. All the median effects on inflation components are virtually the same as in normal times but for some starting conditions the magnitude becomes twice bigger (+2bps of inflation trend, −4bps of 1y IRP). Again, we find a positive correlation between monetary policy shocks and inflation expectations. However, the overall effect on real yields is positive, since inflation expectation increase by only a tenth of the shock, and the response of the IRP is negative. Accordingly, probabilities to go back to a binding ELB go down by 15 percentage points and the effect on ELB risk premium is positive, emphasizing that agents were not expecting the ELB to be binding for long. Lifting off during the 2009-2011 period could not generate sufficiently a large escape to the deflation trap, nor provide a reduction in real rates to stimulate the economy.

The second type of effects can be observed during the anchored ELB period, between 2012 and 2015, where most effects are either dampened or reversed. An initial tightening shock of a few basis points quickly goes back to an undershooting of the short-term by up to 15bps, that is back to the ELB. Long-term yields go down as well by about 10bps, mostly through the expectation component, creating a steepening of the curve. This shock produces deflationary pressure up to −2bps, and effects on inflation risk premia are reversed as well. Inflation volatility goes

up persistently up to 12bps annualized after 5 years, emphasizing the higher inflation uncertainty. Last, ELB probabilities overshoot after 1y by up to 15 percentage points, and ELB risk premia become negative emphasizing the ELB desirability.

In sum, this analysis shows that during the anchored ELB period, the optimal policy is to stay at the ELB by consistently undershooting expectations about monetary policy rates if the economy was converging to the steady state. In this case, real rates go down by more than 10bps since nominal rates fall and IRP increases. This effect is slightly dampened by decreased inflation expectations, because the ELB leads to a prolonged deflation period, as emphasized previously. The price to pay is a slightly heightened inflation uncertainty, which does not translate into a positive risk premia response.

4.5 Embracing the lower bound

Why are the effects of monetary policy so different during the first and second half of the ELB period? The shift observed in 2012 roughly corresponds to the period where the 1y ELB probabilities became higher than 90% (see Figure 3, bottom right panel). I have thus called the 2012-2015 period *anchored* since this is the time at which it became apparent to investors that the ELB was here to stay. One unconventional monetary policy event roughly coincides with this anchoring: the start of calendar-based forward guidance (Aug. 2011).

Early on in the crisis, Williams (2009) called for this "embrace" of the lower bound by leaving short-term nominal rates to close to zero values for a substantial amount of time. One way to analyze efficiency of this policy from the investors' point of view is to measure whether staying at the ELB is associated with high or low marginal utility empirically, and look at the ELB event risk premium. For simplicity of exposition, consider that the effective lower bound parameter is null ($\underline{r} = 0$). Using the model estimates, I form the price of an ELB Arrow-Debreu security, providing \$1 if and only if the ELB binds between today and any date $t + n$ in the future. Such a price $P^{(n)}_{elb,t}$

is given by:

$$P_{elb,t}^{(n)} = \mathbb{E}_t^{\mathbb{Q}} \left[\exp\left(-\sum_{i=0}^{n-1} r_{t+i} \right) \times \mathbb{1}\left\{ r_{t+1:t+n} = 0 \right\} \right] = \mathbb{Q}_t \left[r_{t+1:t+n} = 0 \right] . \tag{17}$$

Equation (17) equates the price of the ELB Arrow-Debreu security with the risk-neutral probability to stay at the ELB. In the model, these risk-neutral probabilities are obtained in closed-form and given by the risk-neutral counterpart of Equation (14). Similarly, the price of this bond purging from the risk premium is given by the physical probability to stay at the ELB, i.e. $\mathbb{P}_t \left(r_{t+1:t+n} = 0 \right)$. These physical probabilities are the one fitted by the model consistently with the primary dealer survey data. The ELB risk premium can be defined as:

$$\mathrm{RP}_{elb,t}^{(n)} = \frac{1}{n} \log \left(\frac{\mathbb{Q}_t(r_{t+1:t+n} = 0)}{\mathbb{P}_t(r_{t+1:t+n} = 0)} \right) . \tag{18}$$

This risk premium is positive (negative) when staying at the ELB coincides with states of high (low) marginal utility. I thus interpret a negative risk premium as indicative of the desirability of a binding ELB in the future, or fear of lifting-off, as perceived by investors.

Figure 9 presents the time series of both physical and risk-neutral ELB probabilities for maturities of 1 and 5 years. The risk-neutral probabilities (grey line) are a direct outcome of the model, and present estimates nearly always below their physical counterparts (black lines), for both maturities. I translate these differences into the risk premium estimates using Equation (18) and represent them on the bottom-left panel.

[Insert Figure 9 about here.]

The negative ELB risk premium observed throughout most of the period indicates that investors mostly fear that the central bank will be lifting off in the short and medium run. This component goes as negative as -1 starting in early 2009. The

magnitude is comparable to what is found in the credit risk literature comparing risk-neutral and physical default probabilities of entities, but has opposite sign (Driessen (2004) finds a log-ratio of 0.75 for corporates, and Monfort et al. (2020) find 1.5 for some European sovereigns). This premium becomes positive for a few months before QE2, date at which the premium drops back to the negative territory for good. Consistently with the U.S. economic recovery, the 1y ELB risk premium becomes positive again in late 2014 as investors expect and desire the central bank to increase gradually interest rates.

Figure 9 emphasizes the role that unconventional monetary policy events had in shaping not only investors' anchoring of ELB expectations, but also their view that staying at the ELB was the right thing to do. Most of the shifts observed on panel (b) can be traced to unconventional monetary policy announcements: the ELB premium becomes significantly negative mostly after QE1 and QE2 episodes. As we showed in the previous section, these changes in investors perception can shift their reactions to similar monetary policy shocks, pushing forward the view that central bank communication is central at the lower bound.

Last, I dissect the ELB desirability into its different contributions and ask whether the embrace of the ELB was purely driven by the inflation outcomes uncovered on Figure 4. To obtain the impact of the inflation trend, I recompute the counterfactual ELB Arrow-Debreu price after imposing that $\lambda_t^{(\pi^*)} = 0$. In the same fashion, I obtain the counterfactual price without inflation volatility pricing by restricting $\lambda_t^{(\sigma)} = 0$. For both cases, I also impose that $\lambda_r = 0$ to avoid having pricing of inflation components through short-rate shocks. Denoting the counterfactual ELB risk premia by $\text{RP}_{elb,t}^{(-\pi^*,n)}$ and $\text{RP}_{elb,t}^{(-\sigma,n)}$ respectively, I obtain the contribution of each component by:[10]

$$\text{RP}_{elb,t}^{(\pi^*,n)} = \text{RP}_{elb,t}^{(n)} - \text{RP}_{elb,t}^{(-\pi^*,n)} \qquad \text{and} \qquad \text{RP}_{elb,t}^{(\sigma,n)} = \text{RP}_{elb,t}^{(n)} - \text{RP}_{elb,t}^{(-\sigma,n)}. \tag{19}$$

10. Note that the physical probabilities are not impacted by this change in the prices of risk. The computation performed in Equation (19) is equivalent to computing $\frac{1}{n}\log\left(\frac{\mathbb{Q}_t(r_{t+1:t+n}=0)}{\widetilde{\mathbb{Q}}_t(r_{t+1:t+n}=0)}\right)$, where $\widetilde{\mathbb{Q}}_t$ is the alternative risk-neutral probability.

I present the decomposition of the ELB risk premium at the 1y and 5y maturity on panels (a) and (b) of Figure 10, respectively. Two striking features emerge from the picture. First, the risk premium associated to inflation trend shocks always contribute negatively to the ELB risk premium, both for the 1y and 5y series and consistently throughout the ELB period. However, this component is virtually unaffected by unconventional monetary policy events. Second, the pricing of inflation volatility shocks contributes negatively to the ELB risk premium before late 2011, and positively afterwards, with an order of magnitude at least twice bigger than the contribution of inflation trend. This is particularly blatant for the 5y maturity (panel (b) of Figure 10) where the inflation volatility contribution grows positive after Twist, and the tapering of 2014. Up to late 2011, the two components contribute to nearly half of the observed negative ELB premium.

[Insert Figure 10 about here.]

This result indicates that lifting-off is associated with adverse inflation trend outcomes during the entire ELB period, and adverse inflation outcomes up until late 2011, date at which the fact that the ELB will be binding for at least a year becomes well-anchored. Past that date, inflation components play in opposite ways on the ELB desirability. The low inflation trend still contributes to the desire to stay at the ELB, while the heightened inflation uncertainty pushes investors towards a liftoff. Overall these results support the view that staying at the ELB may restore inflation expectations upwards while increase uncertainty about future inflation, two counteracting effects from the investors' point of view.

5 Conclusion

In this paper, I investigate how asset prices can reveal information about inflation shocks during the effective lower bound period. I provide a new way of modeling both nominal and real yield curves in an affine framework, which allows for the presence

of inflation trend and volatility and is consistent with a persistent lower bound on nominal yields. Relying on a combination of quadratic term structure models and the gamma-zero distribution, the model is able to generate a short-term nominal rate stuck at the ELB for several periods. I show that the model provides closed-form formulas for nominal and real interest rates, interest rate forecasts, inflation forecasts, impulse-response functions, and liftoff probabilities under both physical and risk-neutral measure.

I provide empirical estimates of inflation components at the ELB, and study their interactions with monetary policy shocks in the U.S.. The ELB-consistent estimation combined with bond prices reveal that the ELB coincides with adverse inflation outcomes, i.e. persistently low inflation trend and high inflation volatility, supporting the view that inflation dynamics shifted at the ELB. These outcomes have a large influence on asset prices, and I show that they generate substantial long-run nominal term premia and short-run deflation fears that drive real yields upward. Second, I show that embracing the ELB is beneficial from the investors perspective, since the liftoff is considered as a bad state of the world. Indeed, an impulse-response exercise reveals that lifting-off can create a wide variety of responses depending on the state of the economy and whether investors expectations of a binding ELB are well-anchored. Unconventional monetary policies thus turn out to be a key monetary policy tool during the ELB for shaping these effects of the liftoff.

Acknowledgements

The author thanks Yakov Amihud, Daniel Andrei, Patrick Augustin, David Backus, Laurent Barras, Paul Beaumont, Sebastien Bétermier, Mikhail Chernov, Antonio Diez De Los Rios, Robert Engle, Andras Fulop, Bruno Feunou, Jean-Sébastien Fontaine, Xavier Gabaix, René Garcia, Joseph Haubrich, Leonardo Iania, Eric Mengus, Alain Monfort, Sarah Mouabbi, Fulvio Pegoraro, Florian Pelgrin, Eric Renault, Jean-Paul Renne, Glenn Rudebusch, Olivier Scaillet, Christopher Sims, Robert Whitelaw, Jonathan Wright. The author also thanks participants to the 7^{th} Bundesbank term structure workshop, 12^{th} ESWC conference in Montreal, the 9^{th} CFE international conference,

9^{th} annual SoFiE conference, Barcelona Graduate School of Economics Summer Forum in time series, 69^{th} Econometric society European summer meeting, 3^{rd} Econometric society European winter meeting, NYU-Stern QFE seminar, Brown University econometrics seminar, CREST financial econometrics seminar, Banque de France seminar, students' finance, macroeconomics and econometrics seminars at NYU, and students' finance seminar at Columbia.

References

Abrahams, M., T. Adrian, R. Crump, E. Moench, and R. Yu. 2016. "Decomposing Real and Nominal Yield Curve." *Journal of Monetary Economics.*

Adrian, T., and H. Wu. 2009. *The Term Structure of Inflation Expectations.* Staff Reports 362. Federal Reserve Bank of New York.

Ahn, D.-H., R. F. Dittmar, and A. R. Gallant. 2002. "Quadratic Term Structure Models: Theory and Evidence." *Review of Financial Studies* 15, no. 1 (March): 243–288.

Anderson, N., and J. Sleath. 2001. *New Estimates of the U.K. Real and Nominal Yield Curves.* Working Paper. Bank of England.

Andreasen, M., and A. Meldrum. 2011. *Likelihood Inference in Non-Linear Term Structure Models: The importance of the Zero Lower Bound.* Technical report.

———. 2015. *Market Beliefs about the UK Monetary Policy lift-off Horizon: A No-Arbitrage Shadow-Rate Term Structure Model Approach.* Technical report.

Andreasen, M., and A. Meldrum. 2018. "A Shadow Rate or a Quadratic Policy Rule? The Best Way to Enforce the Zero Lower Bound in the United States." *Journal of Financial and Quantitative Analysis.*

Andreasen, M. M., and B. J. Christensen. 2015. "The SR approach: A new estimation procedure for non-linear and non-Gaussian dynamic term structure models." *Journal of Econometrics* 184 (2): 420–451.

Ang, A., G. Bekaert, and M. Wei. 2008. "The Term Structure of Real Rates and Expected Inflation." *Journal of Finance* 63, no. 2 (April): 797–849.

Ang, A., J. Boivin, S. Dong, and R. Loo-Kung. 2011. "Monetary Policy Shifts and the Term Structure." *Review of Economic Studies* 78, no. 2 (February): 429–457.

Ang, A., and M. Piazzesi. 2003. "A No-Arbitrage Vector Autoregression of Term Structure Dynamics with Macroeconomic and Latent Variables." *Journal of Monetary Economics* 50, no. 4 (May): 745–787.

Aruoba, B., P. Cuba-Borda, and F. Schorfheide. 2017. "Macroeconomic Dynamics Near the ZLB: A Tale of Two Countries." *The Review of Economic Studies* 85, no. 1 (April): 87–118.

Backus, D. K., S. Foresi, and C. I. Telmer. 2001. "Affine Term Structure Models and the Forward Premium Anomaly." *Journal of Finance* 56, no. 1 (February): 279–304.

Barr, D., and J. Y. Campbell. 1997. "Inflation, Real Interest Rates, and the Bond Market: A Study of U.K. Nominal and Index-Linked Bond Prices." *Journal of Monetary Economics* 39:361–383.

Bauer, M. D., and G. D. Rudebusch. 2016. "Monetary Policy Expectations at the Zero Lower Bound." *Journal of Money, Credit and Banking.*

Bianchi, F., L. Melosi, and M. Rottner. 2019. *Hitting the Elusive Inflation Target.* Technical report. NBER working paper.

Branger, N., C. Schlag, I. Shaliastovich, and D. Song. 2016. *Macroeconomic Bond Risks at the Zero Lower Bound.* Technical report.

Breach, T., S. D'amico, and A. Orphanides. 2020. "The Term Structure and Inflation Uncertainty." *Journal of Financial Economics (forthcoming).*

Camba-Mendez, G., and T. Werner. 2017. *The Inflation Risk Premium in the Post-Lehman Period.* Technical report. ECB.

Campbell, J. Y., and R. J. Shiller. 1991. "Yield Spreads and Interest Rate Movements: A Bird's Eye View." *The Review of Economic Studies* 58 (3): 495–514.

Campbell, J. Y., A. Sunderam, and L. M. Viceira. 2017. "Inflation Bets or Deflation Hedges? The Changing Risk of Nominal Bonds." *Critical Finance Review,* no. 6, 263–301.

Carriero, A., S. Mouabbi, and E. Vangelista. 2018. "UK Term Structure Decompositions at the Zero Lower Bound." *Journal of Applied Econometrics* 33 (5): 643–661.

Cheng, P., and O. Scaillet. 2007. "Linear-Quadratic Jump-Diffusion Modeling." *Mathematical Finance* 17 (4): 575–698.

Chernov, M., and P. Mueller. 2012. "The Term Structure of Inflation Expectations." *Journal of Financial Economics,* no. 106, 367–394.

Christensen, J. H., and G. Rudebusch. 2015. "Estimating Shadow-Rate Term Structure Models with Near-Zero Yields." *Journal of Financial Econometrics* 13 (2): 226–259.

Christensen, J. H. E., and J. M. Gillan. 2012. *Could the U.S. Treasury Benefit from Issuing More TIPS.* Technical report. Federal Reserve Bank of San Francisco.

Christiano, L. 2017. *Comment on Cochrane, "Michelson-Morley, Fisher and Occam: The Radical Implications of Stable Quiet Inflation at the Zero Bound".* Technical report. Northwestern University.

Cochrane, J. H. 2017. "Michelson-Morley, Fisher, and Occam: The Radical Implications of Stable Quiet Inflation at the Zero Bound." In *NBER Macroeconomics Annual 2017, volume 32,* by M. Eichenbaum and J. A. Parker, 113–226. University of Chicago Press, June.

Cogley, T., G. Primiceri, and T. Sargent. 2010. "Inflation-Gap Persistence in the U.S." *American Economic Journal: Macroeconomics* 2, no. 1 (January): 43–69.

Coibon, O., and Y. Gorodnichenko. 2011. "Monetary Policy, Trend Inflation and the Great Moderation: An alternative Interpretation." *American Economic Review* 101:341–370.

D'Amico, S., D. H. Kim, and M. Wei. 2018. "Tips from TIPS: The Informational Content of Treasury Inflation-Protected Security Prices." *Journal of Financial and Quantitative Analysis* 53 (1): 395–436.

Dai, Q., and K. J. Singleton. 2000. "Specification Analysis of Affine Term Structure Models." *Journal of Finance* 55, no. 5 (October): 1943–1978.

———. 2002. "Expectation Puzzles, Time-varying Risk Premia, and Affine Models of the Term Structure." *Journal of Financial Economics* 63, no. 3 (March): 415–441.

Darolles, S., C. Gourieroux, and J. Jasiak. 2006. "Structural Laplace Transform and Compound Autoregressive Models." *Journal of Time Series Analysis* 27, no. 4 (July): 477–503.

Debortoli, D., J. Gali, and L. Gambetti. 2020. "On the Empirical (Ir)Relevance of the Zero Lower Bound Constraint." *NBER Macroeconomics Annual.*

Driessen, J. 2004. "Is Default Event Risk Priced in Corporate Bonds?" *Review of Financial Studies.*

Duffee, G. R. 2002. "Term Premia and Interest Rate Forecasts in Affine Models." *Journal of Finance* 57 (1): 405–443.

Ehling, P., M. Gallmeyer, and C. Heyerdahl-Larsen. 2018. "Disagreement about inflation and the yield curve." *Journal of Financial Economics* 127:459–484.

Engle, R. 1982. "Autoregressive Conditional Heteroscedasticity with Estimates of the Variance of United Kingdom Inflation." *Econometrica* 50, no. 4 (July): 987–1007.

Evans, M. D. D. 1998. "Real Rates, Expected Inflation and Inflation Risk Premia." *The Journal of Finance* 53, no. 1 (February).

Fernandez-Villaverde, J., and J. F. Rubio-Ramírez. 2007. "Estimating Macroeconomic Models: A Likelihood Approach." *Review of Economic Studies* 74 (4): 1059–1087.

Feunou, B., J. Fontaine, A. Le, and C. Lundblad. 2015. *Term Structure Modeling when Monetary Policy is Unconventional: A New Approach.* Technical report.

Feunou, B., and J.-S. Fontaine. 2014. "Non-Markov Gaussian Term Structure Models: The Case of Inflation." *Review of Finance* 18:1953–2001.

Filipovic, D., M. Larsson, and A. Trolle. 2017. "Linear-Rational Term Structure Models." *Journal of Finance* 72 (2): 655–704.

Fleckenstein, M., F. A. Longstaff, and H. Lustig. 2017. "Deflation Risk." 30 (8): 2719–2760.

Fleckenstein, M., F. A. Longstaff, and H. Lustig. 2014. "The TIPS Treasury Bond Puzzle." *Journal of Finance* 69 (5): 2151–2197.

Gali, J. 2018. "The State of New Keynesian Economics: A Partial Assessment." *Journal of Economic Perspectives* 32 (3): 87–112.

Gallant, A., P. Rossi, and G. Tauchen. 1993. "Nonlinear Dynamic Structures." *Econometrica* 61 (4): 871–907.

Garcia, J.-A., and A. Poon. 2018. *Trend Inflation and Inflation Compensation.* Technical report. IMF.

Gouriéroux, C., and J. Jasiak. 2006. "Autoregressive Gamma Processes." *Journal of Forecasting* 25:129–152.

Gourio, F., and P. Ngo. 2020. *Risk Premia at the ZLB: A Macroeconomic Interpretation.* Technical report. Chicago Fed.

Grischenko, O. V., and J.-Z. Huang. 2013. "The Inflation Bond Risk Premium: Evidence From the TIPS Market." *The Journal of Fixed Income.*

Gurkaynak, R. S., B. Sack, and J. H. Wright. 2007. "The U.S. Treasury yield curve: 1961 to the Present." *Journal of Monetary Economics* 54, no. 8 (November): 2291–2304.

———. 2010. "The TIPS Yield Curve and Inflation Compensation." *American Economic Journal: Macroeconomics* 2 (1): 70–92.

Haubrich, J., G. Pennacchi, and P. Ritchken. 2012. "Inflation Expectations, Real Rates, and Risk Premia: Evidence from Inflation Swaps." *Review of Financial Studies* 25 (5).

Joslin, S., M. Priebsch, and K. Singleton. 2014. "Risk Premiums in Dynamic Term Structure Models with Unspanned Macro Risks." *Journal of Finance* 69, no. 3 (June): 1197–1233.

Joslin, S., K. J. Singleton, and H. Zhu. 2011. "A New Perspective on Gaussian Dynamic Term Structure Models." *Review of Financial Studies* 24 (3): 926–970.

Kim, D. H., and A. Orphanides. 2012. "Term Structure Estimation with Survey Data on Interest Rate Forecasts." *Journal of Financial and Quantitative Analysis* 47, no. 01 (February): 241–272.

Kim, D. H., and M. Priebsch. 2013. *Estimation of Multi-Factor Shadow-Rate Term Structure Models.* Federal Reserve Board Discussion Paper Series. Federal Reserve Board.

Kim, D. H., and K. J. Singleton. 2012. "Term Structure Models and the Zero Bound: An Empirical Investigation of Japanese Yields." *Journal of Econometrics* 170 (1): 32–49.

King, T. 2019. "Expectation and Duration at the Effective Lower Bound." *Journal of Financial Economics* 134 (3): 736–760.

Kitsul, Y., and J. H. Wright. 2013. "The Economics of Options-Implied Inflation Probability Density Functions." *Journal of Financial Economics* 110 (3): 696–711.

Koop, G., H. Pesaran, and S. Potter. 1996. "Impulse Response Analysis in Nonlinear Multivariate Models." *Journal of Econometrics* 74 (1): 119–147.

Lansing, K. 2020. "Endogenous Forecast Switching Near the Zero Lower Bound." *Journal of Monetary Economics* forthcoming.

Leippold, M., and L. Wu. 2007. "Design and Estimation of Multi-Currency Quadratic Models." *Review of Finance* 11, no. 2 (January): 167–207.

Lemke, W., and A. Vladu. 2016. *Below the zero lower bound – a shadow-rate term structure model for the euro area.* Technical report.

Mertens, T., and J. Williams. 2018. *What to Expect from the Lower Bound on Interest Rates: Evidence from Derivatives Prices.* Technical report. FRBSF.

Moench, E., and A. Vladu. 2018. *A Fine Term Structure Model for Real and Nominal Bonds.* Technical report. Bundesbank (mimeo).

Monfort, A., and F. Pegoraro. 2012. "Asset pricing with Second-Order Esscher Transforms." *Journal of Banking & Finance* 36, no. 6 (June): 1678–1687.

Monfort, A., F. Pegoraro, J.-P. Renne, and G. Roussellet. 2017. "Staying at Zero with Affine Processes: A New Dynamic Term Structure Model." *Journal of Econometrics* 201 (2): 348–366.

———. 2020. "Affine Modeling of Credit Risk, Pricing of Credit Events and Contagion." *Management Science (forthcoming).*

Monfort, A., J.-P. Renne, and G. Roussellet. 2015. "A Quadratic Kalman Filter." *Journal of Econometrics* 187, no. 1 (July): 43–56.

Pericoli, M., and M. Taboga. 2015. *Understanding Policy Rates at the Zero Lower Bound: Insights from a Bayesian Shadow Rate Model.* Technical report. Bank of Italy.

Pflueger, C. E., and L. M. Viceira. 2016. "Handbook of Fixed Income Securities." Chap. Return Predictability in the Treasury Market: Real Rates, Inflation, and Liquidity (10), edited by P. Veronesi. Wiley.

Priebsch, M. 2013. *Computing Arbitrage-Free Yields in Multi-Factor Gaussian Shadow-Rate Term Structure Models.* Technical report. FRB.

Reichlin, L. 2015. *Commentary: Inflation During and After the Zero Lower Bound.* Technical report.

Renne, J.-P. 2014. "A Model of the Euro-Area Yield Curve with Discrete Policy Rates." *Studies in Nonlinear Dynamics and Econometrics* 21 (1).

Roussellet, G. 2015. "Non-Negativity, Zero Lower Bound and Affine Interest Rate Models." PhD diss., Dauphine University.

Sack, B., and R. Elasser. 2004. *Treasury Inflation-Indexed Debt: A Review of the U.S. Experience.* Economic Policy Review. Federal Reserve Bank of New York, May.

Shen, P. 2006. *Liquidity Risk Premia and Breakeven Inflation Rates.* Economic Review. Federal Reserve Bank of Kansas City.

Stock, J. H., and M. W. Watson. 2007. "Has Inflation Become Harder to Forecast?" *Journal of Money, Credit and Banking* 39 (1): 3–34.

Swanson, E. T., and J. C. Williams. 2014. "Measuring the effect of the zero lower bound on Medium- and Longer-Term Interest Rates." *American Economic Review,* no. 104 (10): 3154–3185.

Williams, J. 2009. "Heeding Daedalus: Optimal Inflation and the Zero Lower Bound." *Brookings Papers on Economic Activity,* 1–37.

Wu, J. C., and F. D. Xia. 2016. "Measuring the Macroeconomic Impact of Monetary Policy at the Zero Lower Bound." *Journal of Money, Credit and Banking* 48 (2-3): 253–291.

Figures and Tables

Figure 1: Nominal and real term structures and inflation data

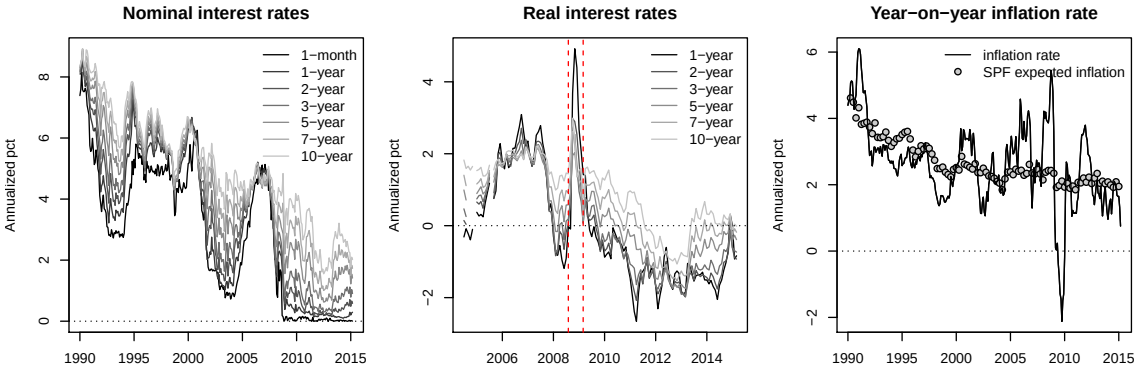

Notes: The left plot presents the time-series of the nominal term structure of interest rates from January 1990 to March 2015. Maturities range from 1 month to 10 years. The middle plot presents the term structure of real rates built as the difference between the nominal zero-coupon interest rates and the inflation swap rates of the same maturity. Observations start in July 2004 and run to March 2015. The vertical red dashed lines indicate the beginning and end of a reduced market liquidity period, that we treat as missing data in the estimation. The right plot presents the realized year-on-year inflation lagged of 3 months (black solid line). The dots superimpose the expected average inflation rate over the next year as measured by the survey of professional forecasters.

Figure 2: Short-rate Simulated Dynamics

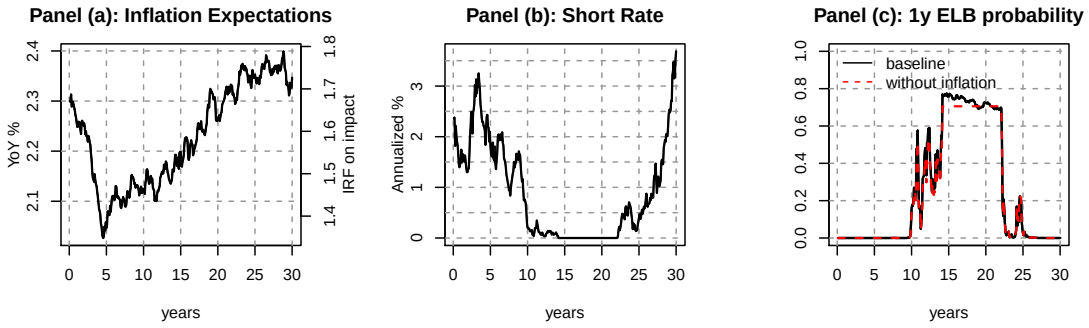

Notes: This figure present 30 years of simulated monthly data from a DGP described by Equation (5) and where parameters are obtained matching moments of inflation and 3m Tbill yield over our sample of estimation. For inflation, inflation squared, and the Tbill yield, we consider means, volatilities, autocorrelations, and cross-correlations. Panel (a) presents the simulated inflation path, panel (b) the short-term nominal interest rate, and panel (c) the implied probability that the ELB will be binding in a year, considering the simulated inflation process (black solid line) or that the inflation is on target (red dashed line). Parameters are: $\alpha = 0.256$, $\phi = 117,500$, $\kappa = -1.0076$, $\beta = 436$, $c = 8.49 \cdot 10^{-6}$, $\mu = 3.31 \cdot 10^{-8}$, $\Phi = 0.999$, $\Sigma = 7.56 \cdot 10^{-11}$.

Figure 3: Fitted series of survey data

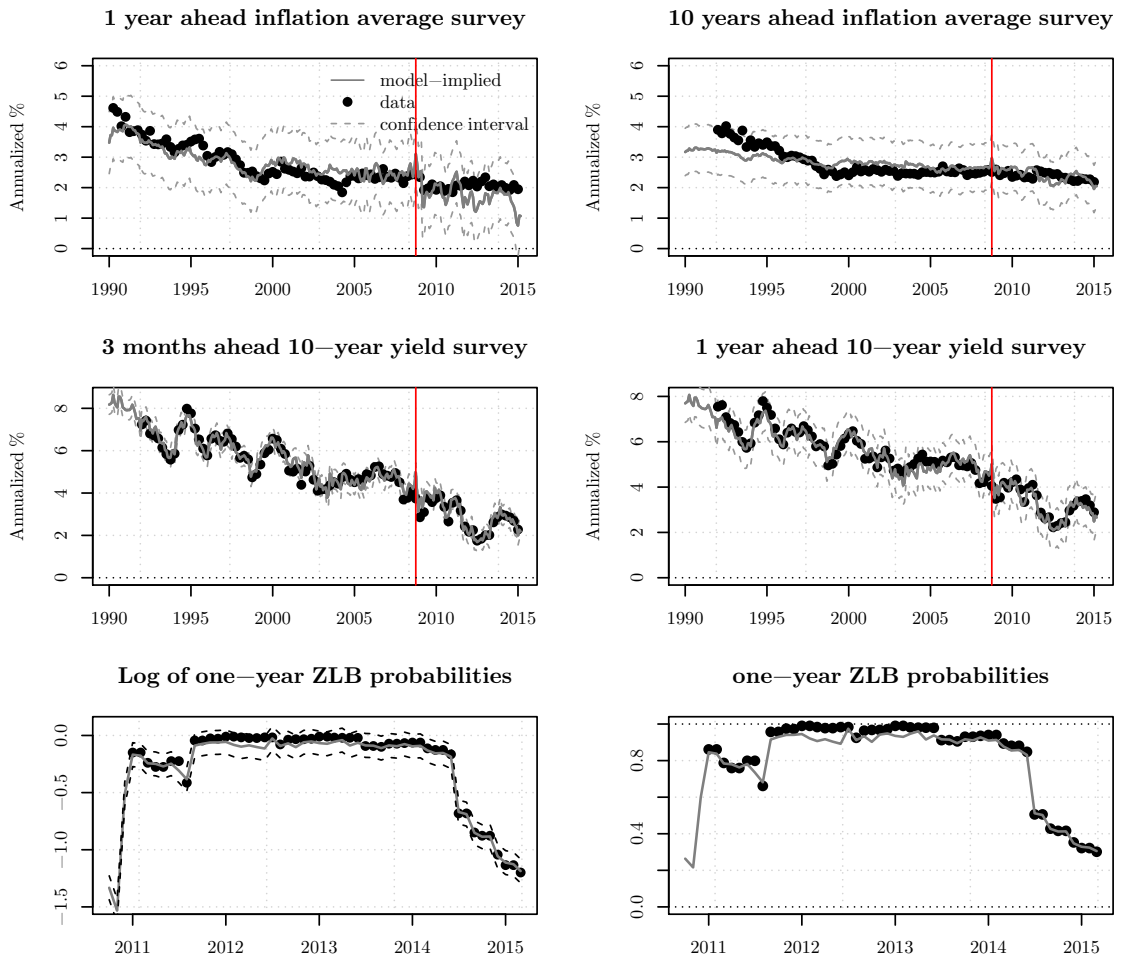

Notes: The black dots correspond to observed forecast data. The grey solid lines correspond to the model-implied forecasted values. Top graphs correspond respectively to the one-year ahead and 10-year ahead inflation average surveys. Medium graphs correspond respectively to the three-months ahead and one-year ahead 10-year yield survey. Units are in annualized percentage points. Bottom graphs correspond respectively to the fitted natural logarithm of ZLB probabilities, and of the exponential of the latter. Confidence intervals computed using the measurement errors standard deviations are plotted in grey dashed lines. The red vertical line delimits the beginning of the zero lower bound period.

Figure 4: Filtered factors

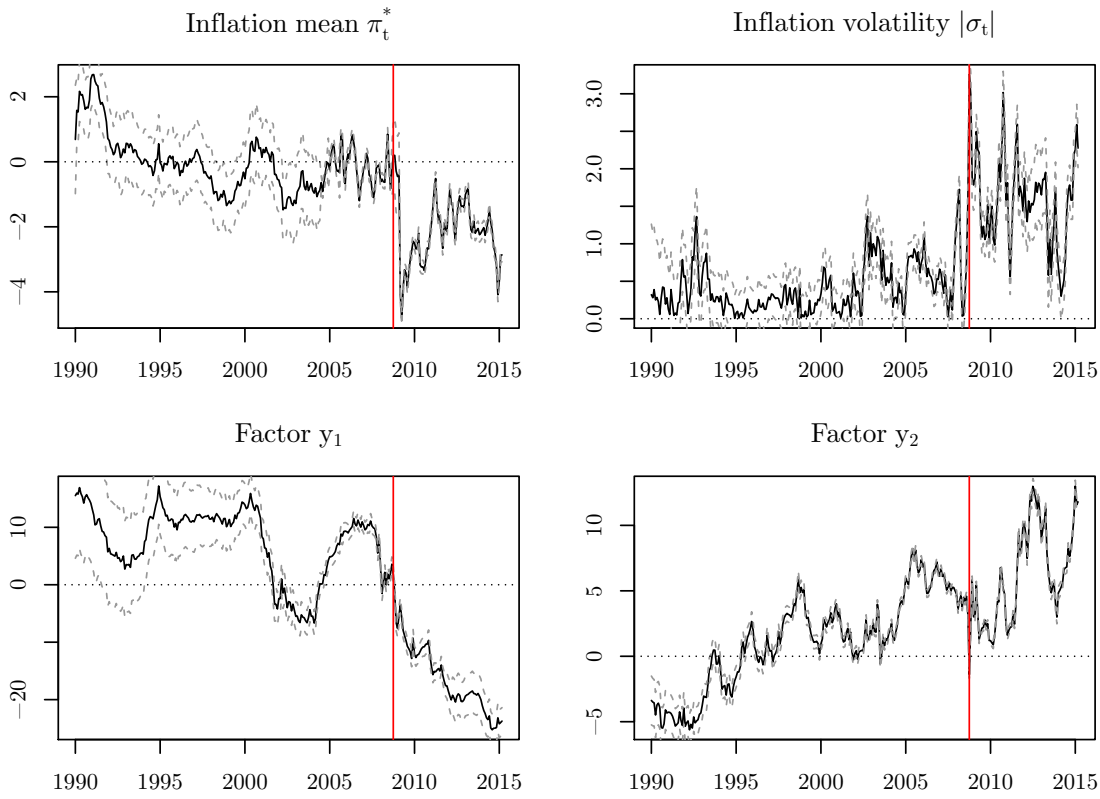

Notes: The unit for inflation central tendency π_t^* and inflation volatility σ_t is in percentage points. Grey dashed lines are 95% confidence bands. The red vertical line delimits the beginning of the zero lower bound period.

Figure 5: Factors loadings of yields

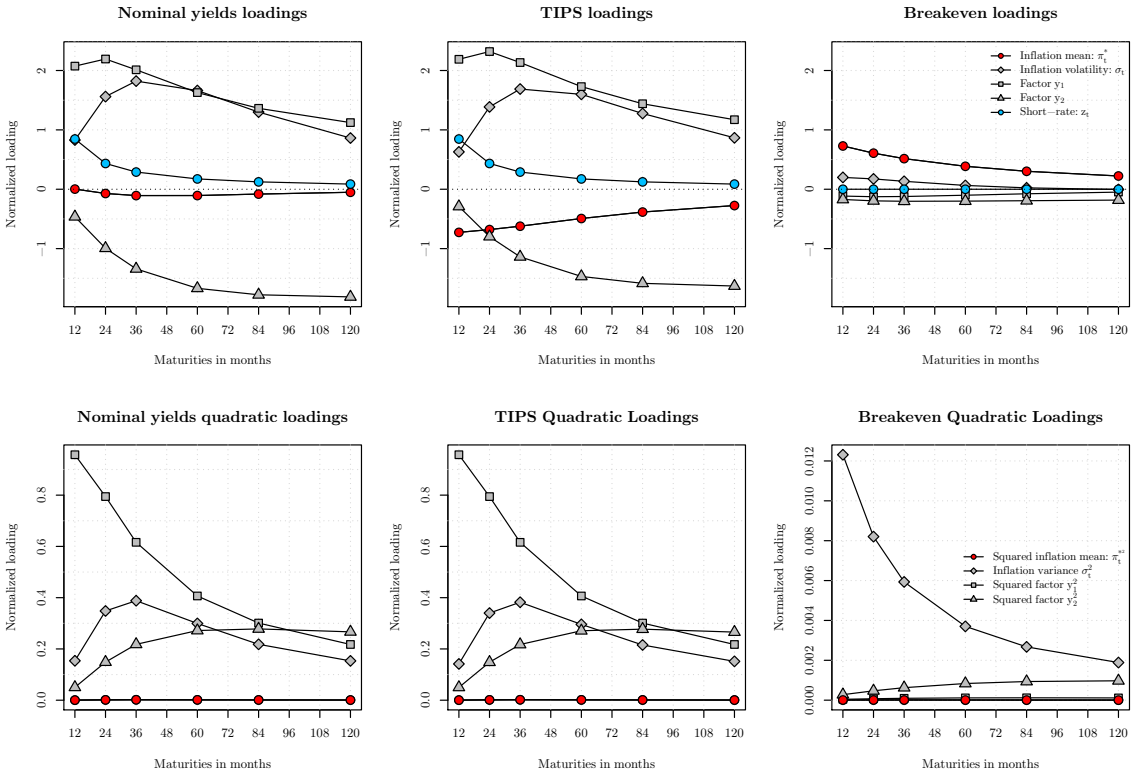

Notes: This plot gathers the linear loadings of the nominal interest rates, of the real rates, and the quadratic loadings with respect to maturity. These loadings are normalized by the in-sample standard deviation of the corresponding filtered factor to be comparable with each other.

Figure 6: Factors loadings of yields components

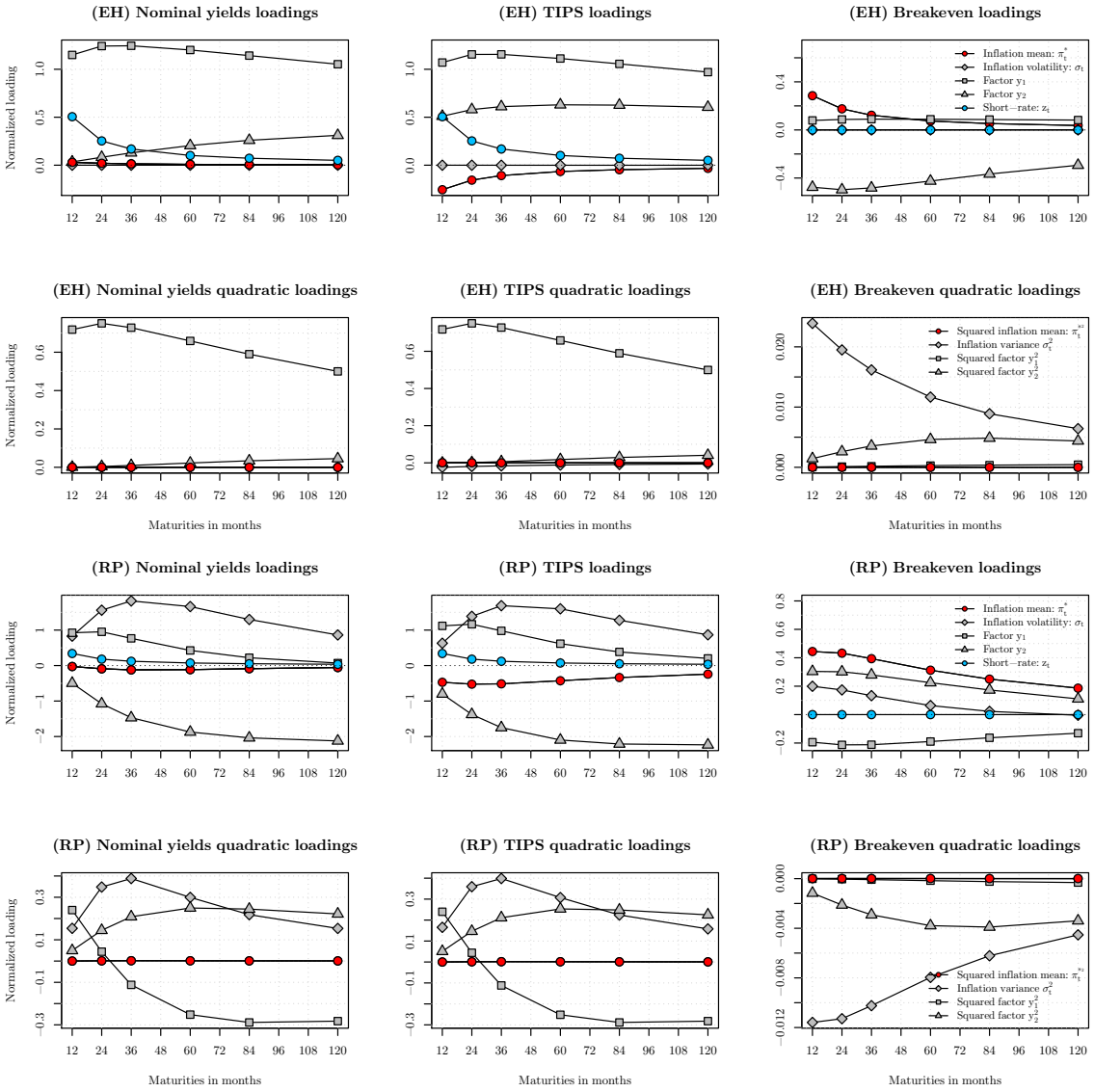

Notes: This plot gathers the linear loadings of the nominal interest rates expectation and risk premia components, of the real rates expectation and risk premia components, and the respective quadratic loadings with respect to maturity. These loadings are normalized by the in-sample standard deviation of the corresponding filtered factor to be comparable with each other.

Figure 7: Decomposition of interest rates

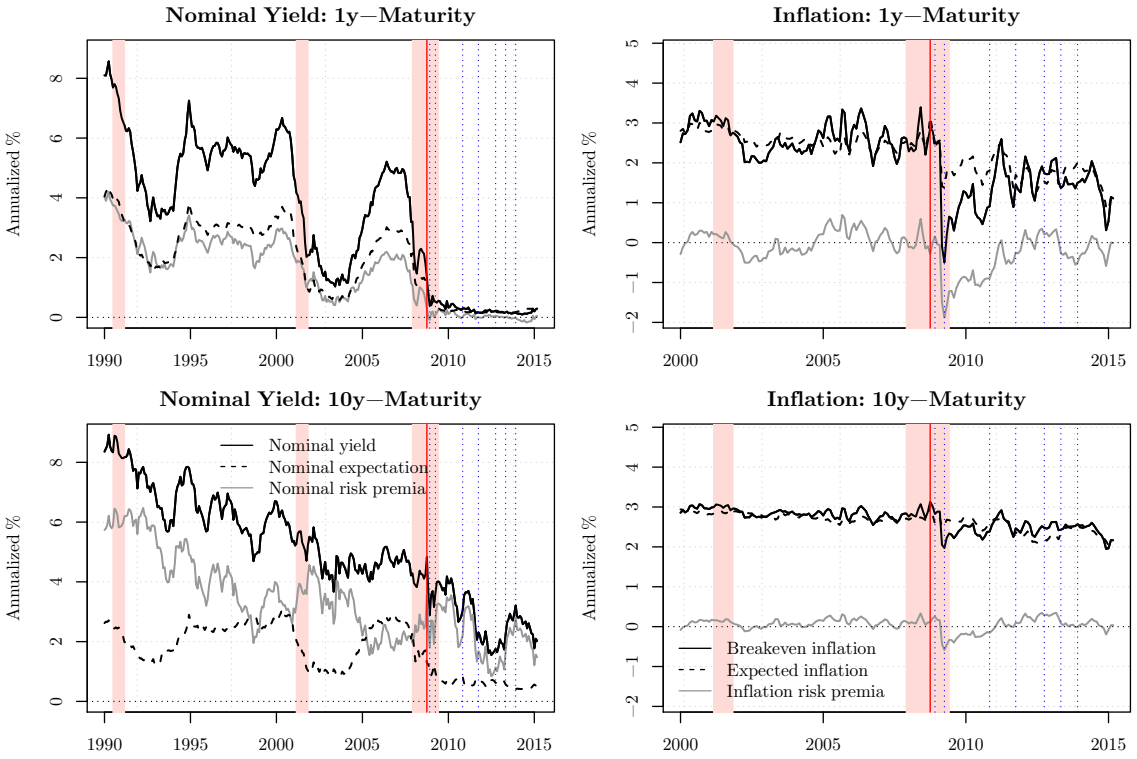

Notes: The first column presents results for the nominal yields components, whereas the second column presents results for the inflation components. The first row presents to the observed data (black solid line), the risk premia (grey solid line), and the expected component (black dashed line) at the one year maturity. The second row presents the same components at the 10 year maturity. Units are in annualized percentage points. The red vertical line delimits the beginning of the zero lower bound period. Pink shaded areas are NBER recession periods. The blue dashed lines are the different unconventional monetary policy episodes, namely: QE1, QE1-extension, QE2, Operation Twist, QE3, Taper tantrum, and the Tapering.

Figure 8: Impulse-response functions: liftoff shock

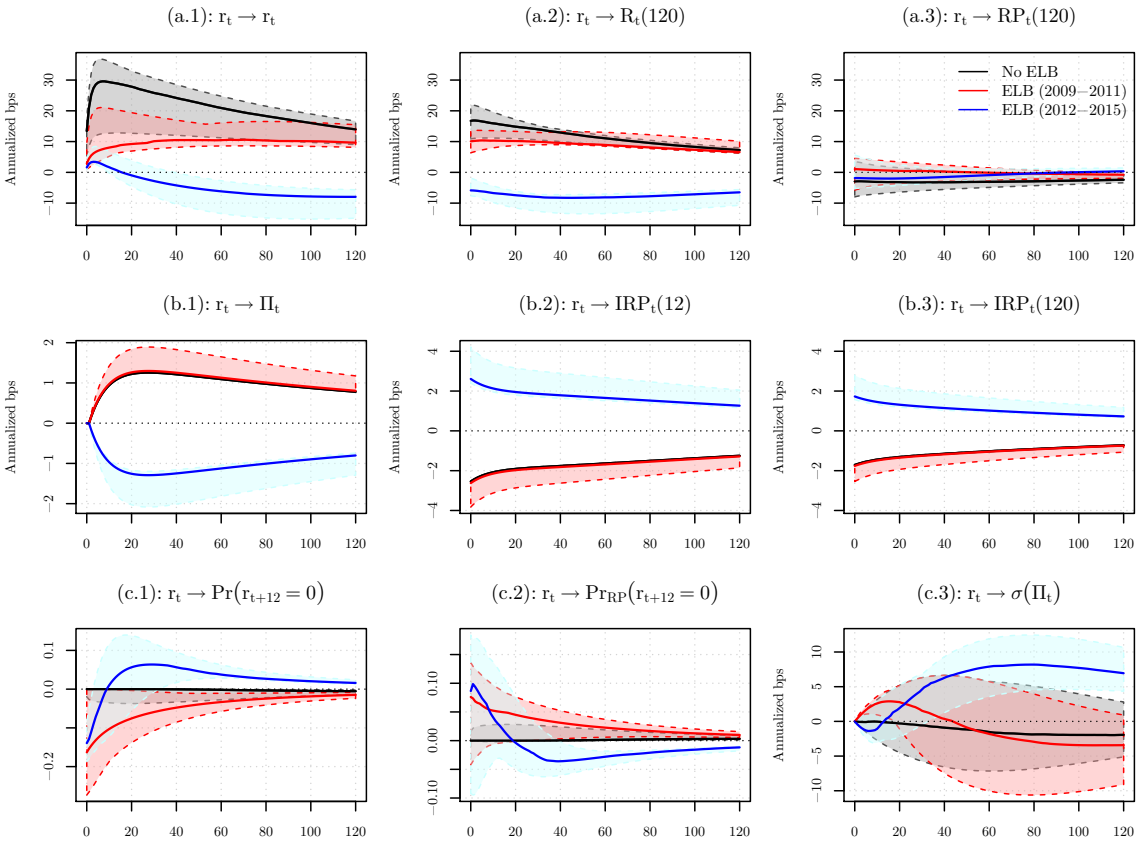

Notes: These graphs present the IRFs of an increase in the short-term nominal interest rate. Panel (a) presents the effect on the nominal side of the term structure, namely the short-term interest rate (a.1), the 10y yield (a.2) and the 10y risk premium (a.3). On panel (b), we find the effects on inflation components, namely inflation itself (b.1), 1y inflation risk premium (b.2) and 10y inflation risk premium (b.3). Panel (c) presents the effects on the 1y ZLB probability (c.1), the 1y ZLB risk premium (c.2) and the inflation volatility (c.3). Grey- and red-shaded areas represent the 50% range of possible outcomes given the different initial values respectively starting from a non-ZLB or a ZLB state. solid lines of the same color are the associated median responses. Green dashed-dotted lines and blue dashed-plus lines respresent the effects of the same shock on particular sample dates, namely on QE2 date and on March 2015 which is the last date of the sample. Units are in annualized basis points.

Figure 9: Physical and risk-neutral liftoff probabilities

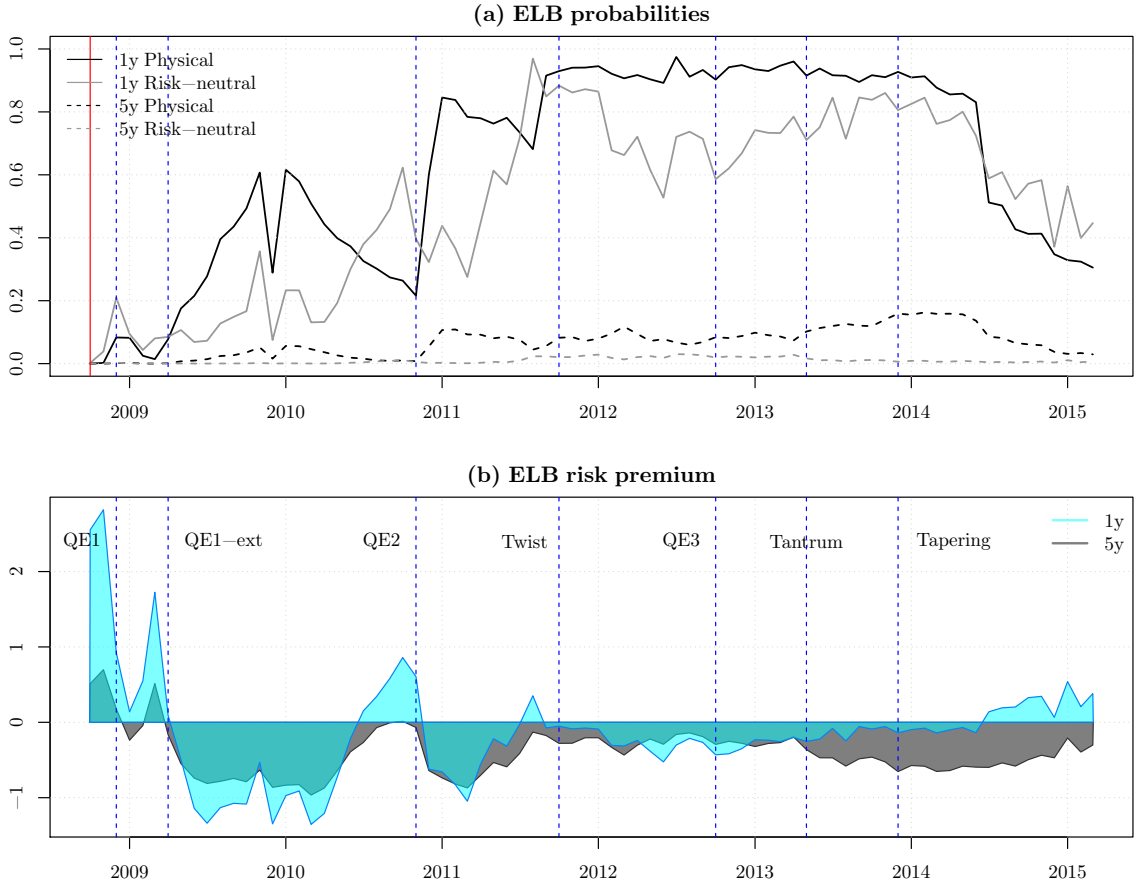

Notes: On panel (a), $\mathbb{P}$- and $\mathbb{Q}$-probabilities are respectively represented with black and grey lines, solid for 1y and dashed for 5y. Panel (b) presents the ELB risk premium as defined by Equation (18), blue for 1y and grey for 5y. All quantities are computed before applying corrections on the factors. The red vertical bar delimits the beginning of the ELB period. The blue dashed lines are the different unconventional monetary policy episodes, namely: QE1, QE1-extension, QE2, Operation Twist, QE3, Taper tantrum, and the Tapering.

Figure 10: Physical and risk-neutral liftoff probabilities without inflation premia

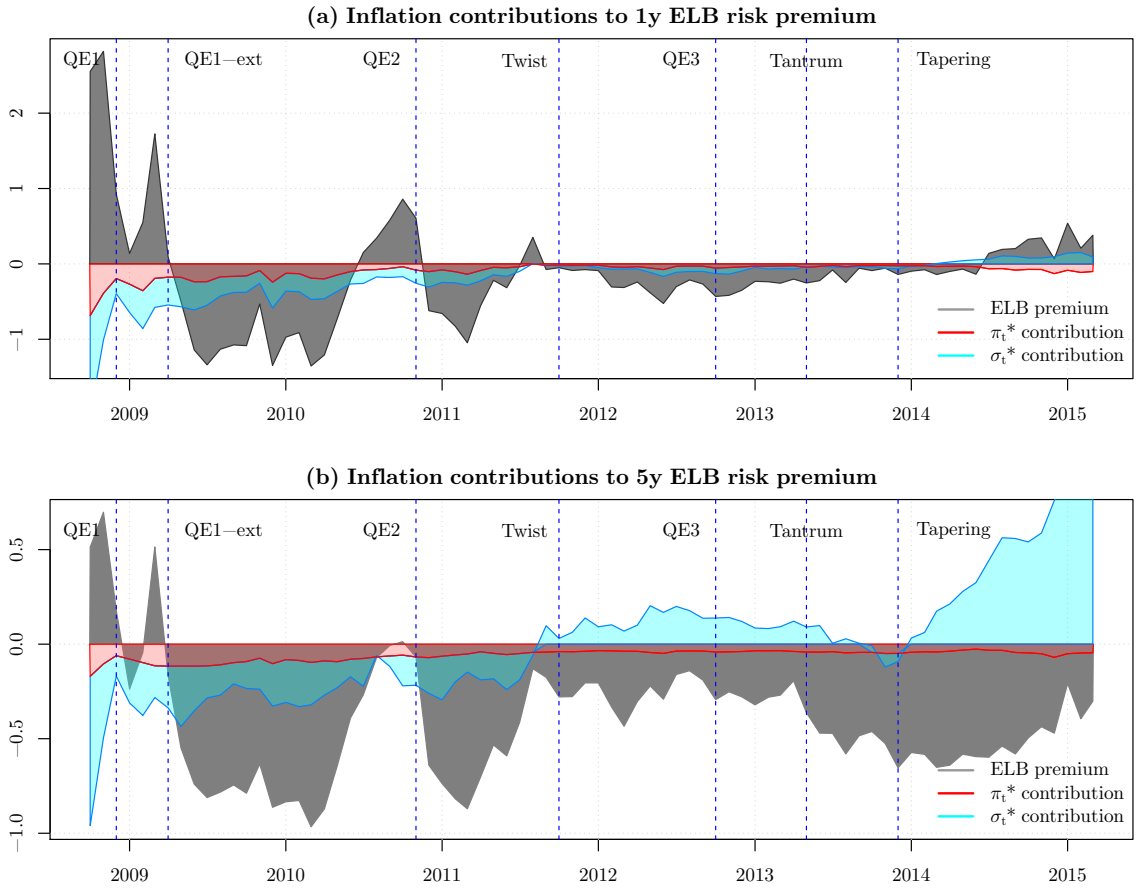

Notes: Both panels presents the ELB risk premium as defined by Equation (18). The red and blue components are the contributions of the inflation trend and volatility to the risk premium. Panel (a) and (b) present the results for the 1y and 5y maturities, respectively. All quantities are computed before applying corrections on the factors. The red vertical bar delimits the beginning of the ELB period. The blue dashed lines are the different unconventional monetary policy episodes, namely: QE1, QE1-extension, QE2, Operation Twist, QE3, Taper tantrum, and the Tapering.

Table 1: Descriptive statistics

	Nominal rates (1990-2015)						
	1-month	1-year	2-year	3-year	5-year	7-year	10-year
mean	2.883	3.375	3.642	3.893	4.336	4.699	5.103
sd	2.228	2.382	2.351	2.272	2.098	1.952	1.800
$\rho(1)$	0.981	0.986	0.985	0.984	0.982	0.980	0.979
	Inflation	Real rates (2004-2015)					
	y-o-y	1-year	2-year	3-year	5-year	7-year	10-year
mean	2.607	-0.071	-0.100	-0.034	0.234	0.532	0.909
mean (excl. crisis)		-0.221	-0.206	-0.111	0.174	0.473	0.855
sd	1.237	1.592	1.423	1.312	1.153	1.069	0.954
sd (excl. crisis)		1.431	1.362	1.286	1.146	1.055	0.936
$\rho(1)$	0.942	0.938	0.963	0.964	0.969	0.962	0.956
		Breakeven inflation rates (2004-2015)					
		1-year	2-year	3-year	5-year	7-year	10-year
mean		1.676	1.858	2.025	2.263	2.421	2.577
mean (excl. crisis)		1.859	1.997	2.130	2.335	2.477	2.615
sd		1.274	0.950	0.759	0.540	0.418	0.303
sd (excl. crisis)		0.886	0.685	0.564	0.414	0.318	0.245
$\rho(1)$		0.855	0.881	0.878	0.877	0.847	0.812

Notes: All units are annualized percentage points. 'mean' are sample averages, 'sd' are sample standard deviations, and '$\rho(1)$' are autocorrelation of order 1. The 'excl. crisis' rows present descriptive statistics calculated on the TIPS data excluding the period from September 2008 to February 2009.

Table 2: Model fit and characteristics

Maturities (months)	1	12	24	36	60	84	120
Nominal rates RMSE (bps)	5.39	4.82	3.60	3.09	2.97	2.61	2.15
Real rates RMSE (bps)	-	17.16	6.02	7.82	10.04	10.61	10.72
Probabilities (in %)	$\mathbb{P}(r_t = \underline{r}) = 27.59$			$\mathbb{P}(r_t = \underline{r} \vert r_{t-1} = \underline{r}) = 74.48$			

Note: Probabilities are calculated with simulated paths of length 100,000.

Parameter Estimates

Table 3: Parameter estimates: X_t dynamics

	estimates	std.		estimates	std.
μ_{π^*}	0.0158^{**}	(0.0072)	$\mu^{\mathbb{Q}}_{\pi^*}$	0.0171^{***}	(0.007)
μ_{σ}	0	–	$\mu^{\mathbb{Q}}_{\sigma}$	0	–
μ_{y_1}	0	–	$\mu^{\mathbb{Q}}_{y_1}$	0.5376^{***}	(0.1683)
μ_{y_2}	0.0217^{**}	(0.0112)	$\mu^{\mathbb{Q}}_{y_2}$	0.0217^{**}	(0.0112)
Φ_{π^*}	0.8855^{***}	(0.0194)	$\Phi^{\mathbb{Q}}_{\pi^*}$	0.9629^{***}	(0.0015)
Φ_{σ,π^*}	0	–	$\Phi^{\mathbb{Q}}_{\sigma,\pi^*}$	0.0043^{***}	(0.0012)
Φ_{y_1,π^*}	0	–	$\Phi^{\mathbb{Q}}_{y_1,\pi^*}$	-0.1256^{***}	(0.0232)
Φ_{y_2,π^*}	0	–	$\Phi^{\mathbb{Q}}_{y_2,\pi^*}$	-0.0195^{***}	(0.0054)
$\Phi_{\pi^*,\sigma}$	0	–	$\Phi^{\mathbb{Q}}_{\pi^*,\sigma}$	0.0169^{***}	(0.0035)
Φ_{σ}	0.9810^{***}	(0.0058)	$\Phi^{\mathbb{Q}}_{\sigma}$	0.9537^{***}	(0.0028)
$\Phi_{y_1,\sigma}$	0	–	$\Phi^{\mathbb{Q}}_{y_1,\sigma}$	0.5023^{***}	(0.0323)
$\Phi_{y_2,\sigma}$	0	–	$\Phi^{\mathbb{Q}}_{y_2,\sigma}$	0.083^{***}	(0.0158)
Φ_{π^*,y_1}	0.0009^{*}	$(5 \cdot 10^{-4})$	$\Phi^{\mathbb{Q}}_{\pi^*,y_1}$	-0.0012^{***}	$(2 \cdot 10^{-4})$
Φ_{σ,y_1}	-0.0006^{***}	$(2 \cdot 10^{-4})$	$\Phi^{\mathbb{Q}}_{\sigma,y_1}$	-0.0006^{***}	$(2 \cdot 10^{-4})$
Φ_{y_1}	0.9944^{***}	(0.001)	$\Phi^{\mathbb{Q}}_{y_1}$	0.9552^{***}	(0.0039)
Φ_{y_2,y_1}	0	–	$\Phi^{\mathbb{Q}}_{y_2,y_1}$	-0.005^{***}	$(8 \cdot 10^{-4})$
Φ_{π^*,y_2}	-0.0142^{***}	(0.0035)	$\Phi^{\mathbb{Q}}_{\pi^*,y_2}$	-0.0043^{***}	$(5 \cdot 10^{-4})$
Φ_{σ,y_2}	0.0078^{***}	(0.002)	$\Phi^{\mathbb{Q}}_{\sigma,y_2}$	0.0036^{***}	$(6 \cdot 10^{-4})$
Φ_{y_1,y_2}	0.0198^{***}	(0.0034)	$\Phi^{\mathbb{Q}}_{y_1,y_2}$	-0.1009^{***}	(0.0065)
Φ_{y_2}	0.9848^{***}	(0.0031)	$\Phi^{\mathbb{Q}}_{y_2}$	0.9848^{***}	(0.0031)
Σ_{π^*}	0.1674^{***}	(0.022)	$\Sigma^{\mathbb{Q}}_{\pi^*}$	0.1674^{***}	(0.022)
Σ_{σ,π^*}	0	–	$\Sigma^{\mathbb{Q}}_{\sigma,\pi^*}$	0	–
Σ_{y_1,π^*}	0	–	$\Sigma^{\mathbb{Q}}_{y_1,\pi^*}$	0.0001^{***}	(0)
Σ_{y_2,π^*}	0	–	$\Sigma^{\mathbb{Q}}_{y_2,\pi^*}$	0	–
Σ_{σ}	0.0999^{***}	(0.0098)	$\Sigma^{\mathbb{Q}}_{\sigma}$	0.0999^{***}	(0.0098)
$\Sigma_{y_1,\sigma}$	0	–	$\Sigma^{\mathbb{Q}}_{y_1,\sigma}$	0	–
$\Sigma_{y_2,\sigma}$	0	–	$\Sigma^{\mathbb{Q}}_{y_2,\sigma}$	0	–
Σ_{y_1}	1	–	$\Sigma^{\mathbb{Q}}_{y_1}$	1.0008^{***}	$(2 \cdot 10^{-4})$
Σ_{y_2,y_1}	0	–	$\Sigma^{\mathbb{Q}}_{y_2,y_1}$	0	–
Σ_{y_2}	1	–	$\Sigma^{\mathbb{Q}}_{y_2}$	1	–

Notes: Standard deviations are in parentheses and are calculated using the outer-product Hessian approximation. The '–' sign indicates that the parameter has been calibrated hence does not possess any standard deviation. Significance level: * <0.1, ** <0.05, *** <0.01.

Table 4: Parameter estimates: short-rate and the prices of risk

	r_t dynamics *(parameters are divided by 1,200 except c, $\bar{\pi}$ and $\underline{r}$)*				
	estimates	std.		estimates	std.
α	1.3317^{***}	(0.4427)	$\alpha^{\mathbb{Q}}$	1.5411^{***}	(0.5345)
β_{π^*}	0.0535^{***}	(0.0165)	$\beta^{\mathbb{Q}}_{\pi^*}$	0.0576^{***}	(0.0176)
β_{σ}	0	–	$\beta^{\mathbb{Q}}_{\sigma}$	0	–
β_{y_1}	0.0901^{***}	(0.0099)	$\beta^{\mathbb{Q}}_{y_1}$	0.0969^{***}	(0.0108)
β_{y_2}	0	–	$\beta^{\mathbb{Q}}_{y_2}$	0	–
κ	1.7071^{***}	(0.2606)	$\kappa^{\mathbb{Q}}$	1.8365^{***}	(0.2928)
ϕ	1.0113^{***}	(0.0894)	$\phi^{\mathbb{Q}}$	1.1704^{***}	(0.0912)
$c \cdot 1200$	0.5471^{***}	(0.0425)	$c^{\mathbb{Q}} \cdot 1200$	0.6331^{***}	(0.0478)
$\underline{r} \cdot 1200$	0.1463^{***}	(0.0035)	$\bar{\pi} \cdot 100$	2.8399^{***}	(0.0601)
	Prices of risk and measurement errors standard deviations				
	estimates	std.		estimates	std.
λ_{0,π^*}	0	–	λ_{0,y_1}	0.524^{***}	(0.1714)
$\lambda_{0,\sigma}$	0	–	λ_{0,y_2}	0	–
λ_{1,π^*}	0.4627^{***}	(0.1045)	λ_{1,π^*,y_1}	-0.0129^{***}	(0.0032)
λ_{1,σ,π^*}	0.0432^{***}	(0.0114)	λ_{1,σ,y_1}	0	–
λ_{1,y_1,π^*}	-0.1259^{***}	(0.0231)	λ_{1,y_1}	-0.0399^{***}	(0.0038)
λ_{1,y_2,π^*}	-0.0195^{***}	(0.0054)	λ_{1,y_2,y_1}	-0.005^{***}	$(8 \cdot 10^{-4})$
$\lambda_{1,\pi^*,\sigma}$	0.1008^{***}	(0.0239)	λ_{1,π^*,y_2}	0.0591^{***}	(0.02)
$\lambda_{1,\sigma}$	-0.273^{***}	(0.0653)	λ_{1,σ,y_2}	-0.0412^{**}	(0.0207)
$\lambda_{1,y_1,\sigma}$	0.5019^{***}	(0.0323)	λ_{1,y_1,y_2}	-0.1206^{***}	(0.0082)
$\lambda_{1,y_2,\sigma}$	0.083^{***}	(0.0158)	λ_{1,y_2}	0	–
λ_r	0.2484^{***}	(0.0588)			
σ_R	0.0208^{***}	$(4 \cdot 10^{-4})$	σ^*_R	0.1184^{***}	(0.0025)
$\sigma^{(12)}_{\pi}$	0.509	–	$\sigma^{(120)}_{\pi}$	0.389	–
$\sigma^{(3)}_{S_R}$	0.231	–	$\sigma^{(12)}_{S_R}$	0.422	–
σ_{ZLB}	0.0522	–			

Notes: Standard deviations are in parentheses and are calculated using the outer-product Hessian approximation. The '–' sign indicates that the parameter has been calibrated hence does not possess any standard deviation. Significance level: * <0.1, ** <0.05, *** <0.01.

A Appendix

A.1 The Gamma-zero (γ_0) distribution

The gamma-zero autoregressive process was introduced by Monfort et al. (2017) as a generalization of the autoregressive gamma process of Gouriéroux and Jasiak (2006). Let $\mathfrak{I}_t = \mathfrak{I}(X_t, z_{t-1})$ be a non-negative process which is a function of the risk factors X_t and z_{t-1}, and j_t be a Poisson variable with intensity $\mathfrak{I}_t$. z_t is conditionally gamma-zero distributed if:

$$j_t|\underline{X_t}, \underline{z_{t-1}} \sim \mathcal{P}\left(\mathfrak{I}(\underline{X_t}, \underline{z_{t-1}})\right) \quad \text{and} \quad z_t|j_t \sim \text{Gamma}_{j_t}(c) \ , \tag{20}$$

that is, conditionally on the Poisson mixing variable, z_t has a gamma distribution with shape (or degree of freedom) parameter j_t and a scale parameter c. When $j_t = 0$, the conditional distribution of z_t converges to a Dirac point mass at zero. Integrating with respect to j_t, we obtain the conditional distribution of z_t given X_t and z_{t-1} that is called gamma-zero, encompassing a zero point mass. The conditional distribution of z_t given X_t and its past can be expressed with its conditional Laplace transform:

$$\mathbb{E}\left[\exp(u_z z_t)\big|\underline{X_t}, \underline{z_{t-1}}\right] = \exp\left(\frac{u_z c}{1 - u_z c}\mathfrak{I}_t\right) \ , \tag{21}$$

In this paper, we consider an intensity which is a linear-quadratic function of X_t and a linear function of z_{t-1} (see Equation (4)). We thus have:

$$\mathbb{E}\left[\exp(u_z z_t)\big|\underline{X_t}, \underline{z_{t-1}}\right] = \exp\left(\frac{u_z c}{1 - u_z c}\left(\alpha + \phi z_{t-1} + \kappa\beta' X_t + (\beta' X_t)^2\right)\right) \ .$$

The properties of the gamma-zero are such that its first two conditional moments are linear in its underlying intensity $\mathfrak{I}_t$. We thus have:

$$\mathbb{E}\left(z_t\big|\underline{X_t}, \underline{z_{t-1}}\right) = c\,\mathfrak{I}_t \quad \text{and} \quad \mathbb{V}\left(z_t\big|\underline{X_t}, \underline{z_{t-1}}\right) = 2\,c^2\,\mathfrak{I}_t \, .$$

We can expand the function of X_t in the intensity:

$$\begin{aligned}
\kappa\beta' X_t + (\beta' X_t)^2 &= \kappa\beta'\left(\mu + \Phi X_{t-1} + v_t\right) + \left[\beta'\left(\mu + \Phi X_{t-1} + v_t\right)\right]^2 \\
&= \kappa\beta'\left(\mu + \Phi X_{t-1} + v_t\right) + \left\{\left[\beta'\left(\mu + \Phi X_{t-1}\right)\right]^2 + \left(\beta' v_t\right)^2 + 2\beta'\left(\mu + \Phi X_{t-1}\right)\beta' v_t\right\} \\
&= \kappa\beta'\mu + \left(\beta'\mu\right)^2 + \beta'\Sigma\beta \\
&\quad + \kappa\beta'\Phi X_{t-1} + \left(\beta'\Phi X_{t-1}\right)^2 + 2\left(\beta'\mu\right)\left(\beta'\Phi X_{t-1}\right) \\
&\quad + \kappa\beta' v_t + \left[\left(\beta' v_t\right)^2 - \beta'\Sigma\beta\right] + 2\left(\mu + \Phi X_{t-1}\right)'\beta\beta' v_t
\end{aligned}$$

Using the conditional moments of linear-quadratic Gaussian processes (see technical Appendix B.5), the last row has zero conditional mean given the information available at $t-1$. We can then express the intensity as:

$$\begin{aligned}
\mathfrak{I}_t &= \alpha + \phi z_{t-1} + \left(\kappa + \beta'\mu\right)\beta'\mu + \beta'\Sigma\beta + \left(\kappa + 2\mu'\beta\right)\beta'\Phi X_{t-1} + \left(\beta'\Phi X_{t-1}\right)^2 \\
&\quad + \kappa\beta' v_t + \left[\left(\beta' v_t\right)^2 - \beta'\Sigma\beta\right] + 2\left(\mu + \Phi X_{t-1}\right)'\beta\beta' v_t\,,
\end{aligned}$$

and the short-rate is given by:

$$\begin{aligned}
r_t &= \underline{r} + c\,\mathfrak{I}_t + \varepsilon_t^z \\
&= \underline{r} + c\,\mathbb{E}_{t-1}\left(\mathfrak{I}_t\right) + \varepsilon_t^r \\
&= \underline{r} + c\left[\alpha + \phi z_{t-1} + \left(\kappa + \beta'\mu\right)\beta'\mu + \beta'\Sigma\beta + \left(\kappa + 2\mu'\beta\right)\beta'\Phi X_{t-1} + \left(\beta'\Phi X_{t-1}\right)^2\right] + \varepsilon_t^r \\
&= \underline{r} + \underbrace{c\left[\alpha + \left(\kappa + \beta'\mu\right)\beta'\mu + \beta'\Sigma\beta\right]}_{=\alpha^*} + \underbrace{c\phi}_{=\phi^*} z_{t-1} + c\left(\kappa + 2\mu'\beta\right)\beta'\Phi X_{t-1} + c\left(\beta'\Phi X_{t-1}\right)^2 + \varepsilon_t^r\,,
\end{aligned}$$

and by definition we obtain:

$$r_t = (1-\phi^*)\underline{r} + \alpha^* + \phi^* r_{t-1} + c\left(\kappa + 2\mu'\beta\right)\beta'\Phi X_{t-1} + c\left(\beta'\Phi X_{t-1}\right)^2 + \varepsilon_t^r\,, \qquad (22)$$

and

$$\varepsilon_t^r = c\left[\kappa\beta' v_t + \left[\left(\beta' v_t\right)^2 - \beta'\Sigma\beta\right] + 2\left(\mu + \Phi X_{t-1}\right)'\beta\beta' v_t\right] + \varepsilon_t^z\,. \qquad (23)$$

This shock is a zero-mean martingale difference with respect to the information set available at $t-1$. For conditional variance, we have:

$$\begin{aligned}
\mathbb{V}_{t-1}(r_t) &= \mathbb{V}_{t-1}(\varepsilon_t^r) \\
&= c^2\mathbb{V}_{t-1}\left[\left(\kappa + 2(\mu+\Phi X_{t-1})'\beta\right)\beta' v_t + \left((\beta' v_t)^2 - \beta'\Sigma\beta\right)\right] + \mathbb{V}_{t-1}(\varepsilon_t^z) \\
&= c^2\left(\left[\kappa + 2(\mu+\Phi X_{t-1})'\beta\right]^2 \beta'\Sigma\beta + 2(\beta'\Sigma\beta)^2\right) \\
&\quad + 2c^2\left(\alpha + \phi z_{t-1} + (\kappa+\beta'\mu)\beta'\mu + \beta'\Sigma\beta + (\kappa + 2\mu'\beta)\beta'\Phi X_{t-1} + (\beta'\Phi X_{t-1})^2\right),
\end{aligned}$$

which is a linear-quadratic function of X_{t-1}.

A.2 Risk-neutral affine property

To derive the risk-neutral conditional Laplace transform of f_t given $\underline{f_{t-1}}$, we use the transition formulas provided in Roussellet (2015), Chapter 4. Using the block recursive affine structure of f_t, the risk-neutral conditional Laplace transform of z_t given X_t and $\underline{f_{t-1}}$ is given by:

$$\begin{aligned}
\mathbb{E}^{\mathbb{Q}}\left(\exp\{u_z z_t\}\middle| X_t,\, \underline{f_{t-1}}\right) &= \frac{\mathbb{E}\left(\exp\{[u_z+\lambda_r]z_t\}\middle| X_t,\, \underline{f_{t-1}}\right)}{\mathbb{E}\left(\exp\{\lambda_r z_t\}\middle| X_t,\, \underline{f_{t-1}}\right)} \\
&= \exp\left\{\left(\frac{(u_z+\lambda_r)c}{1-(u_z+\lambda_r)c} - \frac{\lambda_r c}{1-\lambda_r c}\right)(\alpha + \kappa\beta' X_t + X_t'\beta\beta' X_t + \phi z_{t-1})\right\},
\end{aligned} \tag{24}$$

where $\mathbb{E}^{\mathbb{Q}}(\cdot)$ is the expectation operator under the risk-neutral measure. The difference of ratios can be simplified as follows.

$$\begin{aligned}
\frac{(u_z+\lambda_r)c}{1-(u_z+\lambda_r)c} - \frac{\lambda_r c}{1-\lambda_r c} &= \frac{(1-\lambda_r c)(u_z+\lambda_r)c - [1-(u_z+\lambda_r)c]\lambda_r c}{[1-\lambda_r c][1-(u_z+\lambda_r)c]} \\
&= c\frac{u_z - \lambda_r u_z c + u_z\lambda_r c}{[1-\lambda_r c][1-(u_z+\lambda_r)c]} = \frac{u_z c}{[1-\lambda_r c][1-(u_z+\lambda_r)c]}.
\end{aligned}$$

Define now $c^{\mathbb{Q}} = \dfrac{c}{1-\lambda_r c}$, that is $c = \dfrac{c^{\mathbb{Q}}}{1+\lambda_r c^{\mathbb{Q}}}$. We obtain:

$$\frac{u_z c}{1-(u_z+\lambda_r)c} = \frac{u_z \frac{c^{\mathbb{Q}}}{1+\lambda_r c^{\mathbb{Q}}}}{1-(u_z+\lambda_r)\frac{c^{\mathbb{Q}}}{1+\lambda_r c^{\mathbb{Q}}}} = \frac{1+\lambda_r c^{\mathbb{Q}}}{1-u_z c^{\mathbb{Q}}} \times \frac{u_z c^{\mathbb{Q}}}{1+\lambda_r c^{\mathbb{Q}}} = \frac{u_z c^{\mathbb{Q}}}{1-u_z c^{\mathbb{Q}}}\,.$$

Hence the conditional Laplace transform of Equation (24) is given by:

$$\begin{aligned}\mathbb{E}^{\mathbb{Q}}\left(\exp\{u_z z_t\}\middle| X_t,\, \underline{f_{t-1}}\right) &= \exp\left\{\frac{u_z c^{\mathbb{Q}}}{1-u_z c^{\mathbb{Q}}} \times \frac{\alpha+\kappa\beta' X_t + X_t'\beta\beta' X_t + \phi z_{t-1}}{1-\lambda_r c}\right\} \\ &=: \exp\left\{\frac{u_z c^{\mathbb{Q}}}{1-u_z c^{\mathbb{Q}}}\left(\alpha^{\mathbb{Q}}+\kappa^{\mathbb{Q}}\beta^{\mathbb{Q}\prime} X_t + X_t'\beta^{\mathbb{Q}}\beta^{\mathbb{Q}\prime} X_t + \phi^{\mathbb{Q}} z_{t-1}\right)\right\}.\end{aligned}$$

z_t is therefore conditionally gamma-zero distributed given X_t and its past, where the risk-neutral parameters are given by:

$$\alpha^{\mathbb{Q}} = \frac{\alpha}{1-\lambda_r c}\,,\quad \beta^{\mathbb{Q}} = \frac{\beta}{\sqrt{1-\lambda_r c}}\,,\quad \kappa^{\mathbb{Q}} = \frac{\kappa}{\sqrt{1-\lambda_r c}}\,,\quad \phi^{\mathbb{Q}} = \frac{\phi}{1-\lambda_r c}\,,\quad c^{\mathbb{Q}} = \frac{c}{1-\lambda_r c}$$

We turn now to the computation of the risk-neutral conditional Laplace transform of $(X_t', \mathrm{Vec}(X_t X_t')')'$ given $\underline{f_{t-1}}$. Again, using the property in Roussellet (2015) Chapter 4, we have:

$$\mathbb{E}^{\mathbb{Q}}\left(\exp\left\{u_x' X_t + X_t' U_x X_t\right\}\middle|\underline{f_{t-1}}\right) = \frac{\mathbb{E}\left[\exp\left\{(u_x+\widetilde{\lambda}_{t-1})' X_t + X_t'(U_x+\widetilde{\lambda}_r)X_t\right\}\middle|\underline{f_{t-1}}\right)}{\mathbb{E}\left[\exp\left\{\widetilde{\lambda}_{t-1}' X_t + X_t'(U_x+\widetilde{\lambda}_r)X_t\right\}\middle|\underline{f_{t-1}}\right)},$$

where $\widetilde{\lambda}_{t-1}$ and $\widetilde{\lambda}_r$ are given by:

$$\widetilde{\lambda}_{t-1} = \lambda_0 + \beta\frac{\kappa\lambda_r c}{1-\lambda_r c} + \lambda_1 X_{t-1}\,,\quad \widetilde{\lambda}_r = \frac{\lambda_r c}{1-\lambda_r c}\beta\beta'\,.$$

The transition between the physical and risk-neutral dynamics of X_t are as if the SDF was exponential-quadratic, with adjusted prices of risk $\widetilde{\Lambda}_{t-1}$ and $\widetilde{\lambda}_r$. Since $\widetilde{\lambda}_r$ the price associated to $\mathrm{Vec}(X_t X_t')$ is constant through time, we can rely on the results of Monfort and Pegoraro (2012). We obtain that X_t follows a Gaussian VAR(1) under

the risk-neutral measure and:

$$X_t = \mu^{\mathbb{Q}} + \Phi^{\mathbb{Q}} X_{t-1} + v_t^{\mathbb{Q}}\,,$$

where $v_t^{\mathbb{Q}} \overset{i.i.d.}{\sim} \mathcal{N}\left(0, \Sigma^{\mathbb{Q}}\right)$ is a Gaussian white noise, and $\mu^{\mathbb{Q}}$, $\Phi^{\mathbb{Q}}$ and $\Sigma^{\mathbb{Q}}$ are given by:

$$\begin{aligned}
\mu^{\mathbb{Q}} &= \left(I_K - 2\frac{\lambda_r c}{1-\lambda_r c}\Sigma\beta\beta'\right)^{-1}\left(\mu + \Sigma\lambda_0 + \frac{\kappa\lambda_r c}{1-\lambda_r c}\Sigma\beta\right)\\
\Phi^{\mathbb{Q}} &= \left(I_K - 2\frac{\lambda_r c}{1-\lambda_r c}\Sigma\beta\beta'\right)^{-1}\left(\Phi + \Sigma\lambda_1\right)\\
\Sigma^{\mathbb{Q}} &= \left(I_K - 2\frac{\lambda_r c}{1-\lambda_r c}\Sigma\beta\beta'\right)^{-1}\Sigma\,.
\end{aligned}$$

The class of distributions are thus the same under the physical and the risk-neutral measure. Transforming Formula (37), the risk-neutral Laplace transform of f_t given $\underline{f_{t-1}}$ is given by:

$$\begin{aligned}
&\mathbb{E}^{\mathbb{Q}}\left[\exp\left(u' f_t\right)|\underline{f_{t-1}}\right]\\
=\;& \exp\left\{\frac{u_z c^{\mathbb{Q}}}{1-u_z c^{\mathbb{Q}}}\left(\alpha^{\mathbb{Q}} + \phi^{\mathbb{Q}} z_{t-1}\right) - \frac{1}{2}\log\left|I_K - 2\Sigma^{\mathbb{Q}}\left(U_x + \frac{u_z c^{\mathbb{Q}}}{1-u_z c^{\mathbb{Q}}}\beta^{\mathbb{Q}}\beta^{\mathbb{Q}\prime}\right)\right|\right.\\
+\;& \left(u_x + \frac{\kappa^{\mathbb{Q}} u_z c^{\mathbb{Q}}}{1-u_z c^{\mathbb{Q}}}\beta^{\mathbb{Q}}\right)'\left[I_K - 2\Sigma^{\mathbb{Q}}\left(U_x + \frac{u_z c^{\mathbb{Q}}}{1-u_z c^{\mathbb{Q}}}\beta^{\mathbb{Q}}\beta^{\mathbb{Q}\prime}\right)\right]^{-1}\left[\mu^{\mathbb{Q}} + \frac{1}{2}\Sigma^{\mathbb{Q}}\left(u_x + \frac{\kappa^{\mathbb{Q}} u_z c^{\mathbb{Q}}}{1-u_z c^{\mathbb{Q}}}\beta^{\mathbb{Q}}\right)\right]\\
+\;& \mu^{\mathbb{Q}\prime}\left(U_x + \frac{u_z c^{\mathbb{Q}}}{1-u_z c^{\mathbb{Q}}}\beta^{\mathbb{Q}}\beta^{\mathbb{Q}\prime}\right)\left[I_K - 2\Sigma^{\mathbb{Q}}\left(U_x + \frac{u_z c^{\mathbb{Q}}}{1-u_z c^{\mathbb{Q}}}\beta^{\mathbb{Q}}\beta^{\mathbb{Q}\prime}\right)\right]^{-1}\mu^{\mathbb{Q}}\\
+\;& \left[\left(u_x + \frac{\kappa^{\mathbb{Q}} u_z c^{\mathbb{Q}}}{1-u_z c^{\mathbb{Q}}}\beta^{\mathbb{Q}}\right)' + 2\mu^{\mathbb{Q}\prime}\left(U_x + \frac{u_z c^{\mathbb{Q}}}{1-u_z c^{\mathbb{Q}}}\beta^{\mathbb{Q}}\beta^{\mathbb{Q}\prime}\right)\right]\left[I_K - 2\Sigma^{\mathbb{Q}}\left(U_x + \frac{u_z c^{\mathbb{Q}}}{1-u_z c^{\mathbb{Q}}}\beta^{\mathbb{Q}}\beta^{\mathbb{Q}\prime}\right)\right]^{-1}\Phi^{\mathbb{Q}} X_{t-1}\\
+\;& \left.X_{t-1}'\Phi^{\mathbb{Q}\prime}\left(U_x + \frac{u_z c^{\mathbb{Q}}}{1-u_z c^{\mathbb{Q}}}\beta^{\mathbb{Q}}\beta^{\mathbb{Q}\prime}\right)\left[I_K - 2\Sigma^{\mathbb{Q}}\left(U_x + \frac{u_z c^{\mathbb{Q}}}{1-u_z c^{\mathbb{Q}}}\beta^{\mathbb{Q}}\beta^{\mathbb{Q}\prime}\right)\right]^{-1}\Phi^{\mathbb{Q}} X_{t-1}\right\}. \qquad (25)
\end{aligned}$$

This conditional Laplace transform is an exponential-affine function of f_{t-1}. (f_t) is therefore an affine process under the risk-neutral measure. Combined with the fact that both r_t and π_t are affine functions of f_t augmented with the idiosyncratic inflation shocks ε_t^{π}, this is sufficient to define an affine term structure model (ATSM) (see e.g. Dai and Singleton (2000) or Darolles et al. (2006)).

A.3 Pricing recursions

In this Section, we derive the pricing recursions for nominal bonds and TIPS. By no-arbitrage, we have:

$$P_t^{(n)} = \mathbb{E}_t^{\mathbb{Q}}\left[e^{-r_t} P_{t+1}^{(n-1)}\right] \quad \text{and} \quad P_t^{(n)^*} = \mathbb{E}_t^{\mathbb{Q}}\left[e^{-r_t} P_{t+1}^{(n-1)^*} \frac{\text{CPI}_{t+1}}{\text{CPI}_t}\right]$$

We postulate the form given by Equation (13), that is:

$$\begin{aligned} P_t^{(n)} &= \exp\left(\mathcal{A}_n + \mathcal{B}_n' X_t + X_t' \mathcal{C}_n X_t + \mathcal{D}_n z_t\right), \\ P_t^{(n)^*} &= \exp\left(\mathcal{A}_n^* + \mathcal{B}_n^{*\prime} X_t + X_t' \mathcal{C}_n^* X_t + \mathcal{D}_n^* z_t\right), \end{aligned}$$

Focusing first on nominal bonds, we obtain:

$$\mathcal{A}_n + \mathcal{B}_n' X_t + X_t' \mathcal{C}_n X_t + \mathcal{D}_n z_t = -\underline{r} - z_t + \mathcal{A}_{n-1} + \log \mathbb{E}_t^{\mathbb{Q}}\left[\exp\left(\mathcal{B}_{n-1}' X_{t+1} + X_{t+1}' \mathcal{C}_{n-1} X_{t+1} + \mathcal{D}_{n-1} z_{t+1}\right)\right]$$

Therefore, using the formulation of Equation (25), starting from initial conditions $\mathcal{A}_0 = 0$, $\mathcal{B}_0 = 0$, $\mathcal{C}_0 = 0$, $\mathcal{D}_0 = 0$, we get:

$$\begin{aligned}
\mathcal{A}_n &= -\underline{r} + \mathcal{A}_{n-1} + \frac{\mathcal{D}_{n-1} c^{\mathbb{Q}}}{1 - \mathcal{D}_{n-1} c^{\mathbb{Q}}} \alpha^{\mathbb{Q}} - \frac{1}{2} \log \left| I_K - 2\Sigma^{\mathbb{Q}} \left(\mathcal{C}_{n-1} + \frac{\mathcal{D}_{n-1} c^{\mathbb{Q}}}{1 - \mathcal{D}_{n-1} c^{\mathbb{Q}}} \beta^{\mathbb{Q}} \beta^{\mathbb{Q}\prime}\right)\right| \\
&+ \left(\mathcal{B}_{n-1} + \frac{\kappa^{\mathbb{Q}} \mathcal{D}_{n-1} c^{\mathbb{Q}}}{1 - \mathcal{D}_{n-1} c^{\mathbb{Q}}} \beta^{\mathbb{Q}}\right)' \left[I_K - 2\Sigma^{\mathbb{Q}} \left(\mathcal{C}_{n-1} + \frac{\mathcal{D}_{n-1} c^{\mathbb{Q}}}{1 - \mathcal{D}_{n-1} c^{\mathbb{Q}}} \beta^{\mathbb{Q}} \beta^{\mathbb{Q}\prime}\right)\right]^{-1} \left[\mu^{\mathbb{Q}} + \frac{1}{2} \Sigma^{\mathbb{Q}} \left(\mathcal{B}_{n-1} + \frac{\kappa^{\mathbb{Q}} \mathcal{D}_{n-1} c^{\mathbb{Q}}}{1 - \mathcal{D}_{n-1} c^{\mathbb{Q}}} \beta^{\mathbb{Q}}\right)\right] \\
&+ \mu^{\mathbb{Q}\prime} \left(\mathcal{C}_{n-1} + \frac{\mathcal{D}_{n-1} c^{\mathbb{Q}}}{1 - \mathcal{D}_{n-1} c^{\mathbb{Q}}} \beta^{\mathbb{Q}} \beta^{\mathbb{Q}\prime}\right) \left[I_K - 2\Sigma^{\mathbb{Q}} \left(\mathcal{C}_{n-1} + \frac{\mathcal{D}_{n-1} c^{\mathbb{Q}}}{1 - \mathcal{D}_{n-1} c^{\mathbb{Q}}} \beta^{\mathbb{Q}} \beta^{\mathbb{Q}\prime}\right)\right]^{-1} \mu^{\mathbb{Q}} \\
\mathcal{B}_n &= \Phi^{\mathbb{Q}\prime} \left[I_K - 2\Sigma^{\mathbb{Q}} \left(\mathcal{C}_{n-1} + \frac{\mathcal{D}_{n-1} c^{\mathbb{Q}}}{1 - \mathcal{D}_{n-1} c^{\mathbb{Q}}} \beta^{\mathbb{Q}} \beta^{\mathbb{Q}\prime}\right)\right]^{-1'} \\
&\times \left[\left(\mathcal{B}_{n-1} + \frac{\kappa^{\mathbb{Q}} \mathcal{D}_{n-1} c^{\mathbb{Q}}}{1 - \mathcal{D}_{n-1} c^{\mathbb{Q}}} \beta^{\mathbb{Q}}\right) + 2 \left(\mathcal{C}_{n-1} + \frac{\mathcal{D}_{n-1} c^{\mathbb{Q}}}{1 - \mathcal{D}_{n-1} c^{\mathbb{Q}}} \beta^{\mathbb{Q}} \beta^{\mathbb{Q}\prime}\right)' \mu^{\mathbb{Q}}\right] \\
\mathcal{C}_n &= \Phi^{\mathbb{Q}\prime} \left(\mathcal{C}_{n-1} + \frac{\mathcal{D}_{n-1} c^{\mathbb{Q}}}{1 - \mathcal{D}_{n-1} c^{\mathbb{Q}}} \beta^{\mathbb{Q}} \beta^{\mathbb{Q}\prime}\right) \left[I_K - 2\Sigma^{\mathbb{Q}} \left(\mathcal{C}_{n-1} + \frac{\mathcal{D}_{n-1} c^{\mathbb{Q}}}{1 - \mathcal{D}_{n-1} c^{\mathbb{Q}}} \beta^{\mathbb{Q}} \beta^{\mathbb{Q}\prime}\right)\right]^{-1} \Phi^{\mathbb{Q}} \\
\mathcal{D}_n &= \frac{\mathcal{D}_{n-1} c^{\mathbb{Q}}}{1 - \mathcal{D}_{n-1} c^{\mathbb{Q}}} \phi^{\mathbb{Q}} - 1 .
\end{aligned}$$

Now, turning to TIPS, there is a slight subtlety associated with the fact that π_{t+1} defines the year-on-year inflation and not the monthly inflation rate. The simplest case arises for maturities that are multiple of 12, (yearly maturities), which we have

in the observables. In this case, the price of a TIPS with maturity $n = 12\widetilde{n}$ is given by:

$$P_t^{(12\widetilde{n})^*} = \mathbb{E}_t^{\mathbb{Q}}\left[\exp\left(-\sum_{i=0}^{12\widetilde{n}-1} r_{t+i}\right)\frac{\text{CPI}_{t+12\widetilde{n}}}{\text{CPI}_t}\right] = \mathbb{E}_t^{\mathbb{Q}}\left[\exp\left(-\sum_{i=0}^{12\widetilde{n}-1} r_{t+i}\right)\exp\left(\sum_{j=1}^{\widetilde{n}}\pi_{t+12j}\right)\right].$$

The pricing formulas are still closed-form but rely on the recursions given by the multi-horizon Laplace transform of the vector $f_t^{(aug)} = \left(X_t^{(aug)'},\, X_t^{(aug)'} \otimes X_t^{(aug)'},\, z_t\right)$ and $X_t^{(aug)} = \left(X_t',\, \varepsilon_t^{\pi},\, \pi_{t-1}^*\right)'$. We obtain:

$$P_t^{(12\widetilde{n})^*} = \exp\left(\widetilde{n}\bar{\pi} - 12\widetilde{n}\underline{r} - z_t\right)\mathbb{E}_t^{\mathbb{Q}}\left[\exp\left(\sum_{i=1}^{12\widetilde{n}} u_i' f_{t+i}^{(aug)}\right)\right], \tag{26}$$

where

$$u_{12\widetilde{n}} = \begin{pmatrix} \iota'_{K+2,K+2} & \iota'_{K+1,(K+2)^2} & 0 \end{pmatrix}' \tag{27}$$

$$u_i = \begin{pmatrix} \mathbf{0}'_{K+2} & \mathbf{0}'_{(K+2)^2} & -1 \end{pmatrix}' \quad \text{for} \quad i < 12\widetilde{n} \quad \text{and} \quad i/12 \neq \lfloor i/12 \rfloor \tag{28}$$

$$u_i = \begin{pmatrix} \iota'_{K+2,K+2} & \iota'_{K+1,(K+2)^2} & -1 \end{pmatrix}' \quad \text{for} \quad i < 12\widetilde{n} \quad \text{and} \quad i/12 = \lfloor i/12 \rfloor \tag{29}$$

where $\iota_{i,j}$ is the ith column of the identity matrix of size j. The recursions for the multi-horizon Laplace transform is detailed in the technical Appendix B.4.

A.4 Liftoff probabilities

Using the properties of the gamma-zero process presented in Monfort et al. (2017), the probabilities for the short-term interest rate to stay at its lower bound for n periods are given by the following:

$$\mathbb{P}\left(r_{t+1:t+n} = \underline{r} \middle| \underline{f_t}\right) = \mathbb{P}\left(z_{t+1:t+n} = 0 \middle| \underline{f_t}\right) = \lim_{v \to -\infty} \mathbb{E}\left[\exp\left(\sum_{i=1}^{n} v z_{t+i}\right) \middle| \underline{f_t}\right]$$

$$\mathbb{Q}\left(r_{t+1:t+n}=\underline{r}\middle|\underline{f_t}\right) = \mathbb{Q}\left(z_{t+1:t+n}=0\middle|\underline{f_t}\right) = \lim_{v\to-\infty}\mathbb{E}^{\mathbb{Q}}\left[\exp\left(\sum_{i=1}^{n} v z_{t+i}\right)\middle|\underline{f_t}\right] \quad (30)$$

Notice that it is as if we were computing the n-maturity bond price and its respective expected component for a modified short-rate process. If our short-term nominal rate was given by $-vz_t$, this would be exactly the case. We thus only have to use the same pricing recursions as in Appendix A.3 but putting $\underline{r}=0$ and replacing $c^{\mathbb{Q}}$ by $v\to+\infty$. We obtain:

$$\begin{aligned}
\mathbb{Q}\left(r_{t+1:t+n}=\underline{r}\middle|\underline{f_t}\right) &= \exp\left(\mathcal{A}_n^{(\text{elb})}+\mathcal{B}_n^{(\text{elb})'}X_t+X_t'\mathcal{C}_n^{(\text{elb})}X_t+\mathcal{D}_n^{(\text{elb})}z_t\right)\\
\mathbb{P}\left(r_{t+1:t+n}=\underline{r}\middle|\underline{f_t}\right) &= \exp\left(\mathcal{A}_n^{\mathbb{P},(\text{elb})}+\mathcal{B}_n^{\mathbb{P},(\text{elb})'}X_t+X_t'\mathcal{C}_n^{\mathbb{P},(\text{elb})}X_t+\mathcal{D}_n^{\mathbb{P},(\text{elb})}z_t\right).
\end{aligned}$$

where the loadings follow the recursion:

$$\begin{aligned}
\mathcal{A}_n^{(\text{elb})} &= \mathcal{A}_{n-1}^{(\text{elb})}-\alpha^{\mathbb{Q}}-\frac{1}{2}\log\left|I_K-2\Sigma^{\mathbb{Q}}\left(\mathcal{C}_{n-1}^{(\text{elb})}-\beta^{\mathbb{Q}}\beta^{\mathbb{Q}'}\right)\right|\\
&+ \left(\mathcal{B}_{n-1}^{(\text{elb})}-\kappa^{\mathbb{Q}}\beta^{\mathbb{Q}}\right)'\left[I_K-2\Sigma^{\mathbb{Q}}\left(\mathcal{C}_{n-1}^{(\text{elb})}-\beta^{\mathbb{Q}}\beta^{\mathbb{Q}'}\right)\right]^{-1}\left[\mu^{\mathbb{Q}}+\frac{1}{2}\Sigma^{\mathbb{Q}}\left(\mathcal{B}_{n-1}^{(\text{elb})}-\kappa^{\mathbb{Q}}\beta^{\mathbb{Q}}\right)\right]\\
&+ \mu^{\mathbb{Q}'}\left(\mathcal{C}_{n-1}^{(\text{elb})}-\beta^{\mathbb{Q}}\beta^{\mathbb{Q}'}\right)\left[I_K-2\Sigma^{\mathbb{Q}}\left(\mathcal{C}_{n-1}^{(\text{elb})}-\beta^{\mathbb{Q}}\beta^{\mathbb{Q}'}\right)\right]^{-1}\mu^{\mathbb{Q}}\\
\mathcal{B}_n^{(\text{elb})} &= \Phi^{\mathbb{Q}'}\left[I_K-2\Sigma^{\mathbb{Q}}\left(\mathcal{C}_{n-1}^{(\text{elb})}-\beta^{\mathbb{Q}}\beta^{\mathbb{Q}'}\right)\right]^{-1'}\left[\left(\mathcal{B}_{n-1}^{(\text{elb})}-\kappa^{\mathbb{Q}}\beta^{\mathbb{Q}}\right)+2\left(\mathcal{C}_{n-1}^{(\text{elb})}-\beta^{\mathbb{Q}}\beta^{\mathbb{Q}'}\right)'\mu^{\mathbb{Q}}\right]\\
\mathcal{C}_n^{(\text{elb})} &= \Phi^{\mathbb{Q}'}\left(\mathcal{C}_{n-1}^{(\text{elb})}-\beta^{\mathbb{Q}}\beta^{\mathbb{Q}'}\right)\left[I_K-2\Sigma^{\mathbb{Q}}\left(\mathcal{C}_{n-1}^{(\text{elb})}-\beta^{\mathbb{Q}}\beta^{\mathbb{Q}'}\right)\right]^{-1}\Phi^{\mathbb{Q}}\\
\mathcal{D}_n^{(\text{elb})} &= -\phi^{\mathbb{Q}}.
\end{aligned}$$

For the physical probabilities, the recursions are the same replacing the risk-neutral parameters by the physical ones. We deduce the liftoff probabilities, i.e. to see the first interest rate hike in exactly $n+1$ periods.

$$\mathbb{P}\left(r_{t+1:t+n}=\underline{r}, r_{t+n+1}>\underline{r}\middle|\underline{f_t}\right) = \mathbb{P}\left(r_{t+1:t+n}=\underline{r}\middle|\underline{f_t}\right)-\mathbb{P}\left(r_{t+1:t+n+1}=\underline{r}\middle|\underline{f_t}\right).$$

A.5 Impulse Response Methodology

The affine structure of the model makes it easy to perform an impulse response analysis. All the variables considered in this section can be expressed as linear combinations

of f_t components.[11] Let us consider the impact of a shock of size s of variable v_2 on variable v_1, where $v_1 = e'_{v_1} f_t$ and $v_2 = e'_{v_2} f_t$, with e_{v_1} and e_{v_2} vectors weighting and selecting the right entries of f_t depending on the variables of interest. Let us also denote by $\mathcal{E}_v = (e_{v_3}, \cdots, e_{v_q})$ the matrix of $(q-2)$ weighting vectors that define variables $v_j = e'_{v_j} f_t$ that we do not want to shock at the initial period. The impulse response at horizon n, denoted by $\mathcal{IRF}_{t,n}^{v_2 \to v_1}$ is given by:

$$\begin{aligned} \mathcal{IRF}_{t,n}^{v_2 \to v_1} &= \mathbb{E}\left(e'_{v_1} f_{t+n} \middle| \underline{f_{t-1}},\, e'_{v_2}[f_t - \mathbb{E}(f_t|\underline{f_{t-1}})] = s,\, \mathcal{E}'_v[f_t - \mathbb{E}(f_t|\underline{f_{t-1}})] = 0\right) \\ &- \mathbb{E}\left(e'_{v_1} f_{t+n} \middle| \underline{f_{t-1}},\, e'_{v_2}[f_t - \mathbb{E}(f_t|\underline{f_{t-1}})] = 0,\, \mathcal{E}'_v[f_t - \mathbb{E}(f_t|\underline{f_{t-1}})] = 0\right) \end{aligned} \tag{31}$$

Using the semi-strong VAR formulation of Equation (39), the impulse response function $\mathcal{IRF}_{t,n}^{v_2 \to v_1}$ is given by:

$$\begin{aligned} \mathcal{IRF}_{t,n}^{v_2 \to v_1} &= e'_{v_1} \Psi^n \Big[\mathbb{E}\left(f_t \middle| \underline{f_{t-1}},\, e'_{v_2}[f_t - \mathbb{E}(f_t|\underline{f_{t-1}})] = s,\, \mathcal{E}'_v[f_t - \mathbb{E}(f_t|\underline{f_{t-1}})] = 0\right) \\ &- \mathbb{E}\left(f_t \middle| \underline{f_{t-1}},\, e'_{v_2}[f_t - \mathbb{E}(f_t|\underline{f_{t-1}})] = 0,\, \mathcal{E}'_v[f_t - \mathbb{E}(f_t|\underline{f_{t-1}})] = 0\right)\Big], \end{aligned} \tag{32}$$

which only requires filtered values of the factor f_t given initial and observable conditions.

In our empirical exercise, we are in particular interested in shocking components of X_t itself for inflation central tendency or volatility shocks. The IRF of any variable v_1 to one of those structural shocks on $\iota'_i X_t$, ι_i selecting the i^{th} component of X_t is defined by:

$$\mathcal{IRF}_{t,n}^{v_2 \to v_1} = e'_{v_1} \Psi^n \begin{bmatrix} \Sigma^{1/2} & 0 \\ \Gamma_{t-1}\Sigma^{1/2} & \Sigma^{1/2} \otimes \Sigma^{1/2} \\ c\kappa\beta' & c(\beta \otimes \beta)' \end{bmatrix} \begin{bmatrix} s\iota_i \\ s^2 (\iota_i \otimes \iota_i) \end{bmatrix}, \tag{33}$$

11. or equivalently, $f_t^{(aug)}$. we drop the superscript for ease of notation.

where Γ_{t-1} is defined in Appendix B.5. For general linear functions of f_t, the QKF provides a natural procedure to obtain the most probable vector of shocks. Let $\widetilde{\mathcal{B}} = (e_{v_2}, \mathcal{E}_v)$. The computable version of the IRF of Equation (32) is given by:

$$\mathcal{IRF}_{t,n}^{v_2 \to v_1} = e_{v_1}' \Psi^n \left[\text{Vec}^{-1}(\Omega_0 + \Omega f_{t-1}) \widetilde{\mathcal{B}} \left(\widetilde{\mathcal{B}}' \left[\text{Vec}^{-1}(\Omega_0 + \Omega f_{t-1}) \right] \widetilde{\mathcal{B}} \right)^{-1} \begin{pmatrix} s \\ \\ 0 \end{pmatrix} \right]. \tag{34}$$

Again, the terms in the bracket are slightly modified such that $\text{Vec}(XX')_{t|t} = \text{Vec}(X_{t|t}X_{t|t}')$ and $z_{t|t} \geqslant 0$. To understand where Equation (34) comes from, consider the initial conditions f_{t-1} and the shocks are known without errors, so $P_{t-1,t-1} = 0$. Replacing the unknown quantities in Equation (32) by the values given by the QKF, the result is immediately obtained.

So far, we have only considered responses on variables that can be expressed as affine combinations of the extended vector of factors f_t. However, because of the closed-formedness of the conditional Laplace transform of f_t given its past, we can also compute the conditional expectation of any exponential-affine combination of f_t in closed-form. In general this requires the use of the multi-horizon conditional Laplace transform, which we detail in the technical Appendix B.4. In practice, we apply these formulas to obtain the responses of the ELB probabilities and the corresponding premia.

The average IRF can be computed in two different ways. First, we can apply Formula (32) to the initial condition $f_{t-1} = \left[\bar{X}', \left(\bar{X} \otimes \bar{X}\right)', \bar{z}\right]'$, where $\bar{X} := \mathbb{E}(X_t)$ and $\bar{z} = \mathbb{E}(z_t)$.[12] Second, we can simulate many initial conditions f_{t-1} using its marginal distribution, compute the IRFs using Formula (32) for each initial condition, and average over the responses. The two approaches are not equivalent since they flip the order of integration (see for example Gallant et al. (1993) or Koop et al. (1996)).

12. It is worth mentioning that the initial condition $f_{t-1} = [\bar{X}', \text{Vec}(\bar{X}\bar{X}')', \mathbb{E}(z_t)]'$ is different from $f_{t-1} = \mathbb{E}(f_{t-1})$ since $\mathbb{E}[XX'] \neq \mathbb{E}(X)\mathbb{E}(X')$. However, once conditioning by $X_{t-1} = \bar{X}$, it follows directly that $\text{Vec}(X_{t-1}X_{t-1}') = \text{Vec}(\bar{X}\bar{X}')$ with probability one.

We rely on the latter method in Section **??**.